Escuela Técnica Superior de Ingenieros de Telecomunicación.

Grado en **Ingeniería de Tecnologías Específicas de Telecomunicación.**

Mención en Sistemas de Telecomunicación.

Integration and Performance Evaluation of The RAD1 Spectrometer in The RLS ExoMars Simulator.

Autor:

Álvaro González Martín

Tutores:

Guillermo López Reyes *(Co-Tutor)*

Ramón de la Rosa Steinz *(Tutor)*

Valladolid, julio de 2020.

Universidad de Valladolid

(This page intentionally left blank)

(This page intentionally left blank)

INFORMACIÓN ACADÉMICA

TÍTULO	Integration and Performance Evaluation of The RAD1 Spectrometer in The RLS ExoMars Simulator.
AUTOR	Álvaro González Martín
CO-TUTOR	Guillermo López Reyes
TUTOR	Ramón de la Rosa Steinz
DEPARTAMENTO EMPRESA	Unidad Asociada UVa-CSIC-CAB
DEPARTAMENTO ACADÉMICO	Teoría de la Señal y Comunicaciones e Ingeniería Telemática.

COMISIÓN EVALUADORA

PRESIDENTE	Ramón de la Rosa Steinz
SECRETARIO	J. Carlos Aguado Manzano
VOCAL	Ramón J. Durán Barroso
SUPLENTE 1	Patricia Fernández del Reguero
SUPLENTE 2	Alonso Alonso Alonso

(This page intentionally left blank)

Universidad de Valladolid

ACKNOWLEDGEMENTS

(This page intentionally left blank)

RESUMEN Y OBJETIVOS

El presente proyecto fin de grado se enmarca en el desarrollo del espectrómetro Raman RLS del proyecto ExoMars de la Agencia Espacial Europea, que enviará un rover a Marte en el 2022. La unidad Asociada UVa-CSIC-CAB es un grupo de investigación reconocido (GIR ERICA) de la Universidad de Valladolid, dirigido por el investigador principal del instrumento RLS y, en cuya sede, se encuentra el RLS ExoMars Simulator. Este es un sistema desarrollado para automatizar y emular las capacidades analíticas del instrumento RLS en conjunción con el sistema de preparación y distribución de muestras (SPDS) del rover de ExoMars.

En este marco de actuación, el presente proyecto consta de tres fases diferenciadas:

1. Estudio y puesta al día, comprensión y análisis de la problemática, de la teoría de la espectroscopía Raman y la misión ExoMars, así como de los aspectos hardware y software relevantes del simulador ExoMars.
2. Realización de la integración del espectrómetro RAD1 (RAman Demonstrator 1) en la réplica de laboratorio del instrumento RLS, el Simulador ExoMars.
3. Realización de un estudio de funcionamiento y prestaciones de dicho espectrómetro en conjunción con el resto de elementos del simulador, así como la comparación de dichas prestaciones con la configuración previa basada en un espectrómetro comercial.

La fase de integración se ha realizado de forma escalable, de modo que podrían añadirse nuevos espectrómetros en el futuro. A su vez, el tratamiento de datos y la estructura del código anterior han quedado inalterados.

Finalmente, en la fase del estudio de prestaciones, se han llevado a cabo ensayos con ambos espectrómetros mediante el uso de muestras estándares.

Dichos análisis han permitido la obtención de resultados acerca de las prestaciones ofrecidas en ambas configuraciones, comparándolas a su vez con las del instrumento RLS, pudiendo así evaluar la bondad del sistema con las actualizaciones introducidas. Además, el objetivo fundamental del trabajo es hacer del Simulador ExoMars un emulador más realista, acercándose así a las prestaciones presentes en el instrumento RLS de vuelo.

Palabras clave: espectrometría Raman, simulador RLS, misión ExoMars, instrumento RLS.

(This page intentionally left blank)

(This page intentionally left blank)

Universidad de Valladolid

ABSTRACT AND OBJECTIVES

The technical content of this end-of-studies project is encompassed in the framework of the development of the Raman RLS spectrometer, part of the ExoMars project of the European Space Agency, which is programmed to launch a rover to the Martian surface in 2022. The Associate Unit UVa-CSIC-CAB and the ERICA group, which is a recognized investigation group of the University of Valladolid, are responsible for this instrument. This group is directed by the principal investigator of the RLS instrument and the RLS ExoMars Simulator is located in their facilities. This is a system developed to automatize and emulate the analytical capabilities of the RLS instrument in conjunction with the SPDS (Samples Preparation and Distribution System) of the ExoMars rover.

The aim of this project is well separated into three main objectives:

1. General comprehension of the project, understanding of the basics of Raman spectroscopy and the ExoMars mission, and analysis of the principal hardware/software capabilities of the RLS ExoMars Simulator.
2. Integration of the RAD1 (RAman Demonstrator 1) spectrometer code into the ExoMars Simulator software.
3. Study of the functionalities and the benefits of each spectrometer in conjunction with the rest of the parts of the simulator. Both configurations will be compared to gather data, enabling a technical comparison between spectrometers according to results.

The integration part was accomplished ensuring a scalable structure, in order to allow future code extensions and the incorporation of new spectrometers. At the same time, data treatment and the code structure have remained immutable.

Moreover, as part of the study comparison, standard samples have been used to assure the capabilities of each spectrometer, allowing the analysis of the new actualizations proposed and the final comparison with the real RLS instrument. Finally, the main goal of the project is to improve the realism of the simulator, bringing it closer to the characteristics of the real flying RLS instrument.

Keywords: Raman spectroscopy, ExoMars mission, RLS instrument, RLS ExoMars Simulator.

(This page intentionally left blank)

Universidad de Valladolid

Content

(This page intentionally left blank)

ÍNDICE DE FIGURAS

(This page intentionally left blank)

Universidad de Valladolid

ÍNDICE DE TABLAS

(This page intentionally left blank)

1 Introduction

1.1 Objective: Mars

The robotic exploration of Mars is nowadays fundamental for several reasons, including the prospective of finding organic matter or preparing future manned missions. The Red Planet is the principal candidate to harbor life in our surroundings. For this reason, international space agencies have been working in this field since the late 1990's by sending robotic missions, in a continued effort to understand its environment and conditions and by testing new technologies in preparation of future manned missions.

The decade of 2020 will be very interesting for the exploration of Mars. Some days after the presentation of this work, the NASA Mars 2020 mission will be launched and the Perseverance rover will land on the Jezero crater (Mars) at the beginning of 2021. The same launch window will be used by the Chinese Space Agency to send an orbiter, a lander and a rover all at once, in the Tianwen-1 mission. The following year, in 2022, the Rosalind Franklin rover will be launched to Mars as part of the ExoMars mission.

The ExoMars 2022 mission is a joint effort between the European Space Agency and Roscosmos, the Russian Federal Space Agency. Roscosmos is the launch spacecraft and the landing platform provider, while the ESA is responsible for the rover and the general concept design.

The 2022 rover mission is part of the ExoMars program, which evolved from the Aurora programme, whose primary objective was to create a long-term plan for Europe in terms of robotic, but also human exploration of the Solar system *(Vago et al., 2017)*. The search of life outside our planet was also a foundational key objective. Indeed, the Robotic Exploration of Mars webpage of the ESA states the following main objectives for the mission which, in order of priority, are (*ESA - Robotic Exploration of Mars - Scientific Objectives of the ExoMars Rover*, n.d.):

- Searching for signs of past and present life on Mars surface.

- Characterising the water/geochemical compounds of the visual environment and the underground.
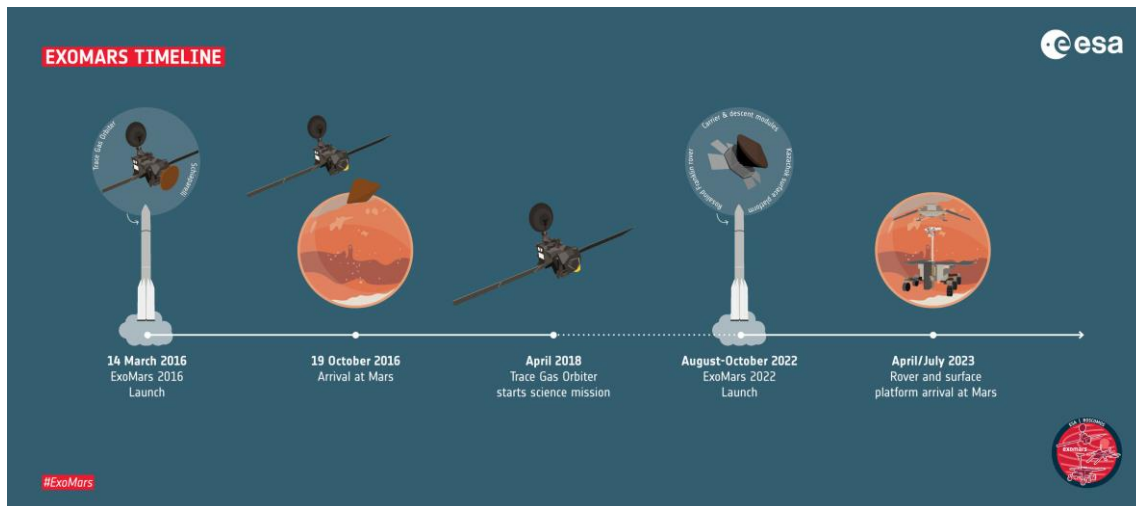
Figure 1. ESA missions for the red planet.

Figure 1 depicts the scheduled missions within the ExoMars program actuation umbrella, with two main phases. The first achieved in 2016 by placing the Trace Gas Orbiter in Mars, which is performing great science and will fulfil a key role as data relay during operations of the 2022 rover mission. The 2016 mission was also fundamental to settle the right path for the landing of the future rover mission, thanks to the valuable lessons-learnt from the failed landing of the Schiaparelli landing demonstrator.

1.2   Looking for evidence of past and present life on Mars

The idea of finding life in Mars is sustained by the belief that, in the past, Mars was much warmer and wetter than it is nowadays. These surface conditions were present on Mars within the first billion years after planetary formation and they were similar to the conditions that allowed the first microbes to gain foothold on planet Earth.

One of the issues of the Earth geochemical analysis is the fact that high-temperature metamorphic processes and tectonic movements have resulted in the reformation of most ancient terrains. Hence, humans have been unable to find mineral formations older than 3.5-4 billion years. On the other hand, Mars did not suffer tectonic movements, which converts the prospective planet in a perfect candidate to analyse old rock formations and to allow researchers to draw a picture of the ancient conditions of Mars (which can be related to the ancient conditions on Earth).

Previous discoveries revealed multiple deposits of salt and clay minerals, reinforcing the idea of finding liquid water, which is another reason to keep investigating on Mars. These discoveries, in this sense, might lead to the understanding of life on our own planet, and may help answering one of the most relevant topics ever, regarding our uniqueness in the Universe. The first ESA advisors, back in 1999 agreed that future missions should be focused on extinct life on Mars; but also, on preparing future missions to have enough flexibility to identify signs of actual life, if present in the current Mars environment.

1.3 The need for subsurface exploration

Effectively identifying chemical biomarkers requires access to well-preserved organic molecules. Nevertheless, some adverse effects on Mars atmosphere complicate this process. The ultraviolet radiation is very high, easily causing damage to organic molecules present on the Martian surface rocks or regolith. The ultraviolet photochemistry produces reactive oxidant species that can destroy biomarkers and, finally, ionising radiation penetrates the Mars atmosphere and could alter organic molecules above the detection sensitivity of scientific devices (*ESA - Robotic Exploration of Mars - Scientific Objectives of the ExoMars Rover*, n.d.).

To overcome these issues successfully, the only way is to look for samples that have been preserved by being protected from the ionizing and UV radiation, which will naturally occur in underground caves or the subsurface. To access this kind of samples, the Rosalind Franklin rover will be equipped with a drill that will take samples from rocks down to 2 meters depth (see concept in Figure 2). This depth is considered enough to ensure a potentially better preservation of the organic molecules that might be present in the rocks. The ExoMars rover is unique in this configuration, as it is the first time that any in situ measurement on Mars will be done in potentially well-preserved samples.
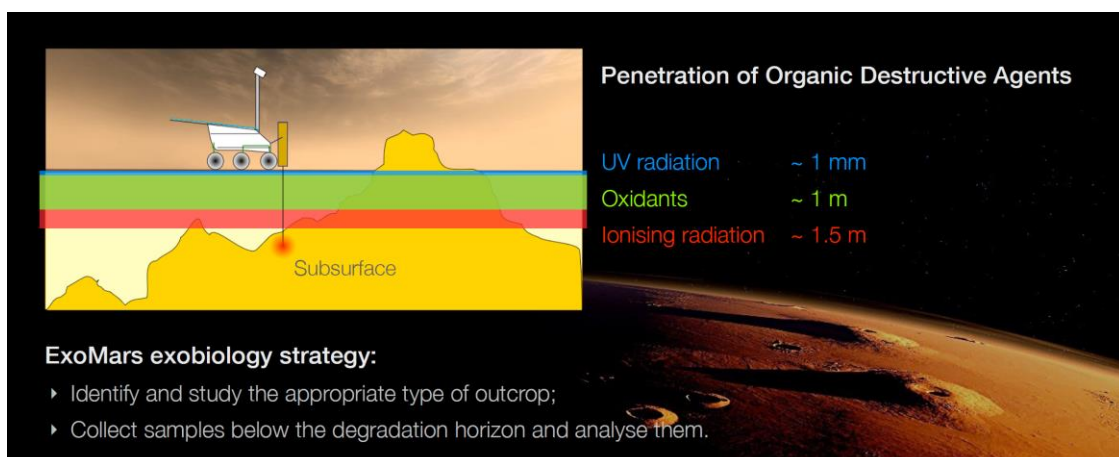
Figure 2. ExoMars rover subsurface sample extraction schematic. Credit: J.Vago (ESA).

1.4 The Rosalind Franklin rover of ExoMars 2022

The ExoMars rover mission will set a new milestone in the European Space Agency history. In order to achieve this endeavour, several European institutions have been involved and collaborated in this mission, establishing an international consortium at all levels of the mission.

The Rosalind Franklin rover, named after the British scientific, will feature a full set of analytical instruments to perform analysis on Martian samples, on a moving laboratory (the rover) that will be able to autonomously navigate the Martian surface. The instruments that are part of the rover payload are the following:

- **PanCam**: A panoramic camera that will provide digital terrain mapping of the Martian surface.
- **ISEM**: The ISEM is an infrared spectrometer that will assist identifying the mineralogical composition of surface targets, working together with the PanCam instrument to contribute to the selection of suitable samples for further analysis with more accurate instruments.
- **CLUPI**: Stands for Close-Up Imager and is a camera system that will acquire high-definition color close-up images of rocks, stones and other types of objects presents in Mars.
- **WISDOM**: A ground-penetration radar to characterise the stratigraphy under the rover.
- **ADRON**: This system will assist searching for subsurface water and hydrated minerals.
- **Ma_MISS**: Located inside the drill, this instrument is expected to be helpful studying mineralogy and rock formation.
- **MicrOmega**: Another kind of infrared imaging spectrometer for mineralogy studies.
- **MOMA**: Mars Organic Molecule Analyser, this device will target biomarkers.

- **RLS Spectrometer**: This instrument is a Raman Spectrometer developed by the University of Valladolid and INTA. It constitutes the framework of this end-of-studies project. The RLS spectrometer will determine the mineralogical composition and identify organic materials in the Martian samples.

The different devices included in the rover (except for the internal instruments) are presented in Figure 3.
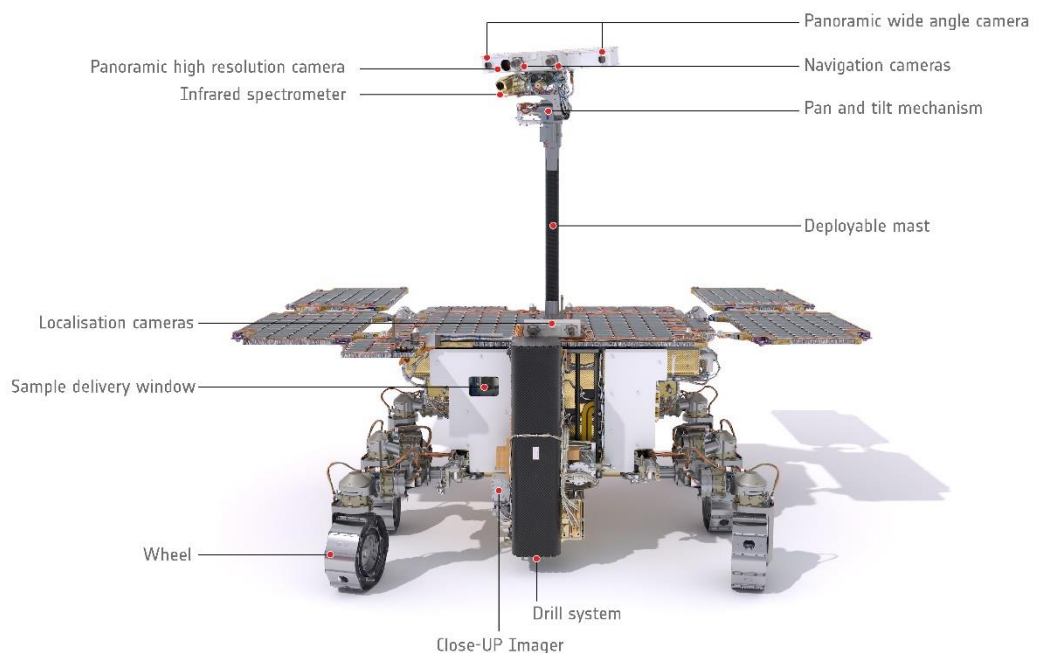
Figure 3. Rosalind Franklin ExoMars 2022 mission rover.

The drill, though not considered an analytical instrument, will be a key device on the rover operations, as it provides access to the subsurface samples to be analysed. The rover will use PanCam, ISEM, ADRON and WISDOM to identify, analyse and select the optimal point for performing an analysis. The drill will then extract the sample, with the Ma_Miss instrument analysing the borehole during drilling. Then CLUPI will image the extracted sample before it is introduced inside the Analytical Laboratory Drawer (ALD).

Universidad deValladolid

Inside the ALD, the sample will be crushed into powder and then delivered by the Sample Preparation and Distribution System (SPDS) for analysis by the three main analytical instruments of the mission: MicrOmega, RLS and MOMA, which will collaboratively analyse the powdered and flattened sample, looking for interesting spots that will be analysed by the three instruments in the same spot. This complex sequence of operations establishes a new paradigm in the robotic operations on Mars. Instead of individual experiments working on separate samples, Rosalind Franklin will require the cooperation among all the instruments and systems of the rover to perform its studies. This has been referred to as "collaborative science" on Mars, aiming at having all the instruments analyzing the same sample, on the very same spots.

The ExoMars rover is expected to perform up to 6 experiments cycles, involving the acquisition and analysis of a surface sample and one subsurface sample, plus 2 vertical surveys, consisting on obtaining five subsurface samples at 50 cm intervals down to 2 meters depth (*ESA - Robotic Exploration of Mars - Scientific Objectives of the ExoMars Rover*, n.d.).

Universidad de Valladolid

2 State of the art

Spectroscopy is a discipline based on the study of the interaction between matter and electromagnetic radiation in form of light and, in order to characterize and identify materials, it uses the measurement of the reflection produced by specific compounds of the material under analysis as a function of wavelength (W.E.S., 1977). Despite this simple functioning, it is important to carefully consider the geometrical and spectral conditions of the surface to be analysed, in other to achieve accurate measurements of the sample.

A general schematic representation of a spectrometer is presented in Figure 4. General Spectrometry schematic (Spectrometer: What Is a Spectrometer? | Types of Spectrometers, n.d.).A laser light is directed towards the sample to be characterised. Therewith, a series of filters are used to guide the photons to the main sample. Light is later directed to a diffraction grating that separates the constitutive light rays according to their primary wavelength. To finish the process, the desirable photons are directed to a CCD board (Charge Coupled Device)[1], transforming the detected light into electrons that can be measured and converted to digital information with an analogic to-digital-converter.
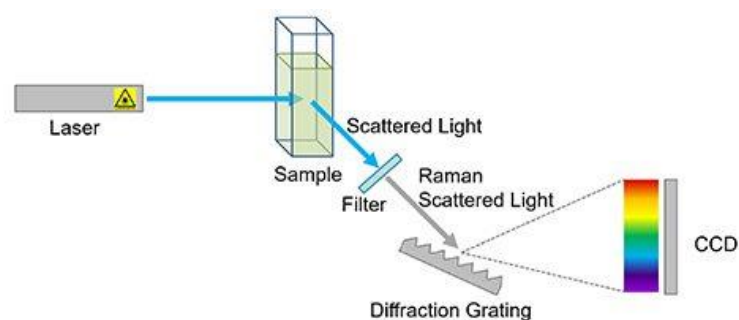
Figure 4. General Spectrometry schematic (Spectrometer: What Is a Spectrometer? | Types of Spectrometers, n.d.).

---

[1] *A CCD is an integrated circuit etched into a silicon surface, forming light sensitive elements which receive the name of pixels. Photons actuating directly towards the CCD surface can be read by an electronic board, creating a digital copy of the information contain on each photon (What Is A CCD?- Charge Coupled Device, n.d.).*

Spectroscopy devices have been used for several decades in research institutions, being Infrared Spectroscopy (IR) the principal and favourite spectroscopy technique for space exploration, due to its reliability and low operation cost. It has been widely used for investigation on Earth, orbiters and in situ instrumentation. This way, IR spectroscopy devices are also **included in the payload of the ExoMars mission** (ISEM, Ma_Miss and MicrOmega instruments use different forms of IR spectroscopy). However, together with this technology, the ESA decided to include a Raman spectroscopy instrument, the RLS instrument. And it is not accidental that the Perseverance rover also includes Raman spectrometers (Sherloc, SuperCam) among its payload instrumentation. The justification of incorporating this technique into the payload on planetary missions results from the following considerations *(Schneider, 1984)*:

- First, technology readiness. The technological advances of the last 20 years have allowed the construction of instruments that can be qualified for space exploration.

- Second, the complementarity between Raman and IR spectroscopies. Some vibrations are only Raman-active while others are only Infrared-active.

- In general, the resolution obtained with Raman allows detecting different phases of the same mineral type (e.g. IR can detect carbonates, and Raman will be able to define which one it is)

- Some vibrations are inherently weak in IR and strong in Raman spectra.

- The diameter of the sample spot for Raman tends to be small (50 microns in RLS, some millimeters in SuperCam…). Therefore, only a tiny sample area is needed to obtain Raman spectra.

- Water is a weak Raman scatterer (though it can be easily detected). Hence, Raman spectra of aqueous samples can be obtained without major interference from water molecules, while IR spectroscopy suffers from the strong absorption of water.

For these reasons, Raman advantages are clear in order to detect biological compounds in samples, even with the presence of water. Besides this clear

advantage, Raman and IR spectroscopy are both applicable to the solid state as well as to gaseous solutions.

2.1 Raman Spectroscopy for the exploration of Mars

Raman Spectroscopy is a chemical analysis technique that provides detailed information about chemical structures and molecular interactions. It is a scattering technique, which means that a laser light source is directed towards a sample. Most of the light scattered by the sample will be emitted with the same wavelength as the excitation laser (receiving the name of Rayleigh Scattering). Nevertheless, some of the absorbed photons will be scattered at slightly different wavelengths due to the vibrations induced by the laser of the molecular bonds in the sample chemical structure. This scattering effect occurs with a probability between 10^{-12} and 10^{-7}. As a result, with proper filtering and collection methods, different chemical structures will scatter the light in different wavelengths, allowing the identification of the mineral structure, thus performing molecular identification of the sample.

The history behind this technique starts in 1928, when Sir Chandrasekhra Venkata Raman discovered the phenomenon that bears his name, and which earned him the Nobel prize *(Ferraro et al., 2003)*. This scattering technique is now known as Raman Spectroscopy. Further developments and contributions transformed the technique into the modern Raman commercial instrumentation known nowadays.

Since its discovery, the Raman spectrometry has been used in various kinds of scenarios and disciplines. Due to its characteristics (fast, non-destructive, non-invasive, clean, accurate…) the technique is applicable in industries such as:

- Pharmaceutical and Cosmetics: The technique has been used for blend uniformity, powder content and purity, contaminant identification and many more.

- <u>Geology and Mineralogy:</u> Used in fluid inclusions, phase transitions, mineral behaviour, gemstone and mineral identification, etc.
- <u>Carbon Materials</u>.
- <u>Semiconductors</u>: To detect purity, doping effects …
- <u>Life sciences</u>: DNA analysis, Bone structure, cell sorting, characterization of bio-molecules, etc. *(Amer, 2010)*

All these characteristics, together with the evolution of the technology, have made Raman Spectroscopy a technique selected by space agencies around the world for Martian exploration. NASA Mars 2020 mission includes two Raman Spectrometers in the Perseverance rover, Sherloc and SuperCam. As for the ESA, the RLS instrument is part of their ExoMars 2022 mission.

This technique is a unique candidate well appreciated by academia and general industry, given that non-destructive methods for characterization will be fundamental for the exploration of Mars. Finally, by using this technique the ESA hopes to obtain valid results, which will be complemented by other results obtained with other devices mounted in the rover, to make decisions into performing destructive (but more accurate) analysis of the samples by the MOMA instrument. All instruments together are expected to lead to promising and encouraging discoveries in the Martian surface with this collaborative science approach, where the Raman spectroscopy will play a key role.

2.1.1 Raman spectrometer and spectra basics

Typically, a Raman spectrometer requires a monochromatic laser source to enable the excitation of the target species, filters and optics to collect the Raman scattered light, diffraction gratings to scatter the Raman light according to wavelength and, finally, collection optics to focus the scattered light on a detector (CCD) to decode the signals into digital data. In this way, a normal Raman spectrum represents in the abscissae axis the Raman shift (wavenumber of the Raman vibration with respect to the laser wavenumber). On the other hand, ideally, photons collected by the CCD are represented as intensity peak in the

ordinate axis. However, the photon/electron conversion in the CCD is usually not 1:1, plus the charge conversion from an analog to a digital signal (with an Analogical/Digital Converter or ADC) is affected by several factors including the bits used for quantifying the signal. This is the reason, together with the relatively low interest in absolute intensity magnitudes in Raman analysis, why typically the Raman spectrum intensity is provided in arbitrary units (a. u.). A typical Raman spectrum is shown in Figure 5.
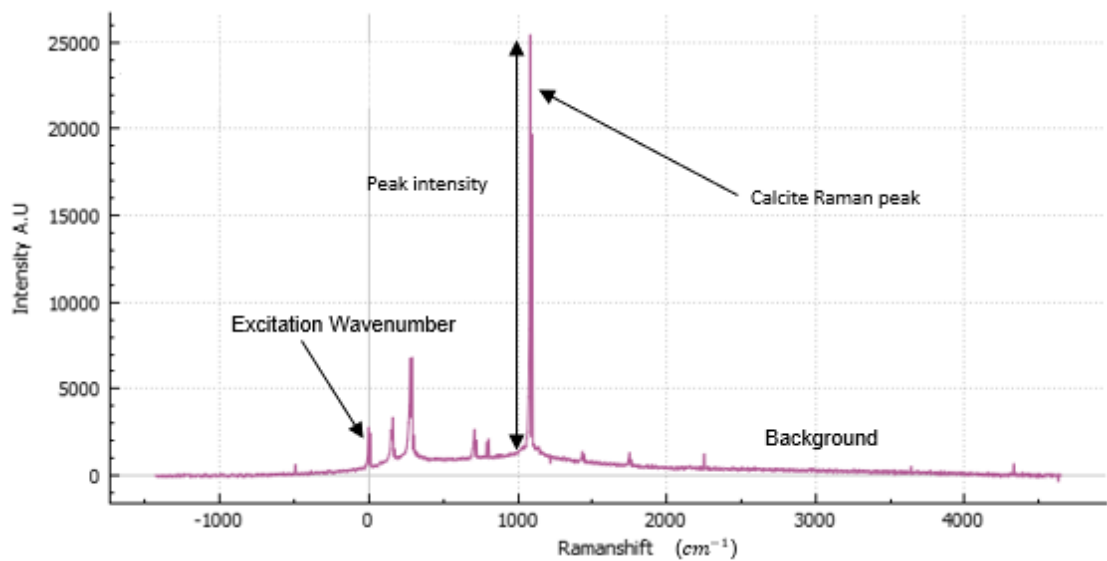
Figure 5. Typical Raman Spectrum (Calcite sample, RAD1).

Depending on the sample under analysis, and the spectrometer efficiency and considering the intrinsic weakness of the Raman effect, it is important to apply acquisition techniques to increase the SNR of a Raman spectrum, which can be done by:

- Optimization of the integration time: The total time the CCD will collect light during an acquisition is referred as integration time (Ti). Even if there are several effects that can impair the spectral quality for higher integration times (related to the dark current of the CCD), the modern spectrometers use CCDs cooled to negative temperatures, making dark current negligible compared to the

acquired signal. In this situation, increasing Ti to cover most the CCD dynamic range (without saturating it), will increase the SNR of the acquired spectrum.

- <u>Calculation of a Dark scan:</u> This initial process is always recommended to reduce the noise or background produced by the presence of spectral artifacts or ambient conditions (such as ambient light). This Dark Scan is simply a spectra acquisition with the same integration time as the spectrum, with the laser turned off. The Dark spectrum is subtracted to the main spectra, reducing in this way the background of the spectrum.

- <u>Spectra accumulation:</u> Usually the maximization of Ti is not enough to obtain a good spectral quality. In this case, to improve the SNR it is possible to perform accumulations. This accumulation process consists in capturing several consecutive spectra with the same integration time (time during which the CCD is capturing photons) that will be later averaged or added (accumulated), allowing the reduction of noise (typically in a factor square root of the number of accumulations) thus improving the final SNR of the acquired spectrum.

Finally, is important to highlight that in a normative Raman spectra representation, the x axis can be represented in different units. These units include Raman shift, wavenumber and wavelength. A complete explanation of each unit is provided here:

- <u>Pixel:</u> Calculations carried out internally by the CCD and computer are in pixel units. In a CCD, the capacitors integrated in the chip represent pixels that are later interpreted by a computer.
- <u>Wavelength:</u> the emission peaks can be represented as function of their emission wavelength in nm.
- <u>Wavenumber:</u> Referred to as the spatial frequency of a wave, the wavenumber is the number of times a wave vibrates in a distance unit. The preferred units are in cm^{-1} for Raman spectra. Equation 1. Wavenumber definition formula. displays the formula to convert wavelength to wavenumber.

$$k = \frac{1}{\lambda}$$

Equation 1. Wavenumber definition formula.

- <u>Raman Shift:</u> These units are the most common ones for Raman spectra. The Raman shift is the difference between the wavenumber of an emission peak with respect to the laser wavenumber, expressed in inverse length (cm^{-1}), because this value is directly related to energy and scales linearly with it. The advantage of this representation is that with these units, the peak positions for a determined Raman emission are constant irrespective of the laser wavelength used for the excitation of the sample. The transformation formula is shown in Equation 2.

$$Raman\ shift\ [cm^{-1}] = \frac{10^7}{\lambda_{ex}[nm]} - \frac{10^7}{\lambda\ [nm]}$$

Equation 2. From wavelength to the Raman shift transformation.

2.2   RLS Instrument

The Raman Laser Spectrometer (RLS) instrument is a Raman spectrometer instrument, part of the Pasteur Payload on board the ExoMars mission to be mounted in the ExoMars 2022 rover. The ERICA group, a recognised research group of the University of Valladolid, as part of the Associated Unit UVa-CSIC-CAB is responsible for the RLS instrument (F. Rull, professor at UVa, is the Principal Investigator). The INTA (Instituto Nacional de Técnica Aeroespacial), the Spanish aerospace research institution, was responsible of designing, qualifying and testing the RLS instrument, which was successfully delivered by the end of 2018 and integrated into the rover in 2019.

This instrument will perform Raman spectroscopies on crushed powdered samples inside what has been called ALD (Analytical Laboratory Drawer) of the Rover, not only contributing to the goal of precise identification of mineral details of the Martian surface, but also to the capability of detecting organic matter if presented on the collected samples.

The RLS instrument consists of the following units (*Raman Laser Spectrometer (RLS) Para Exomars : Estado Actual Raman En ExoMars y Su Evolución*, n.d.):

- **SPU**: SPectrometer Unit for the collection and diffraction of light.
- **iOH**: internal Optical Head to guide the excitation and collection light to and from the sample, also providing autofocus capabilities.
- **ICEU**: Instrument Control and Excitation Unit, including the redundant laser.
- **CT**: Calibration Target. RLS includes two CTs on the rover, to calibrate the spectral position of the instrument, but also to allow alignment between the RLS and MicrOmega fields of view.
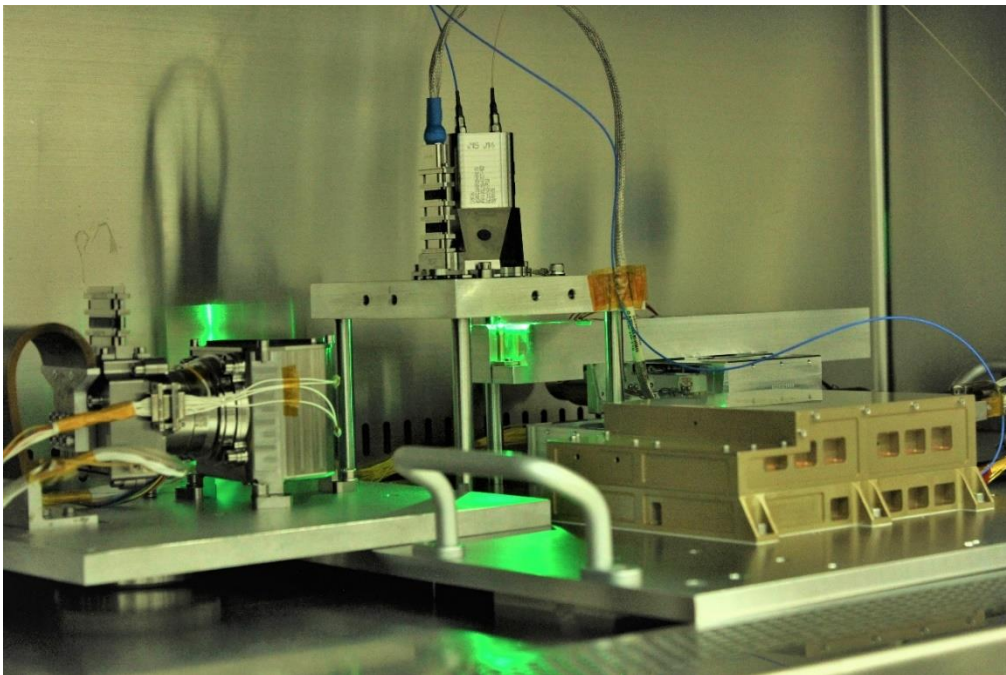
Figure 6. RLS instrument during a test at INTA facilities before delivery.

The instrument features the following Raman-related characteristics (Rull et al., 2018):

- **Laser excitation wavelength**: 532 nm.
- **Irradiance on sample**: 0.6 -1.2 kW/cm^2
- **Spectral range**: 150-3800 cm^{-1} .

- **Spectral resolution**: 6 cm^{-1} lower spectral wavenumbers; 8 cm^{-1} long spectral wavenumbers.
- **Spectral accuracy**: < 1 cm^{-1}.
- **Spot size**: 50 microns.

The principal technical and physical characteristics are (Rull et al., 2018):

- **Mass** of around 2.4 Kg.
- **Power consumption**: 20 W to 30 W (according to the temperature).
- **Full performance:** between -40 ºC and 0ºC.
- Survival **temperatures** between -60º C and +50ºC.
- Redundant laser excitation chain.
- **Storage memory** needed of around 200Mbits for 20 measurements + auxiliary data.
- Active focusing of laser of around ±1 mm range.

The RLS instrument is designed to operate considering two different operation approaches:

- Automatic scanning: the rover shall position the target following a preconfigured sequence of movements (Lopez-Reyes & Rull, 2015). The RLS would take, at this point, a minimum of 20 shots per sample.
- Smart scanning: MicrOmega IR images would be processed by the rover to determine the existence of any interesting target for the RLS instrument. In the hypothetical case of not finding a target of interest, the automatic preconfigured movements would take place instead (Lopez-Reyes & Rull, 2015).

In any case, the rover will be in charge of positioning the samples to the instrument by means of the Sample Preparation and Distribution System (SPDS), which features a carrousel for this purpose.

During the development of instruments for space exploration, several models are manufactured to ensure the final product: breadboards, structural and thermal models (STM), engineering and qualification models (EQM), flight model (FM) -the one to fly- and flight spare (FS) -and exact replica of the FM for redundancy-. Currently, the RLS FS is located at INTA, Torrejón de Ardoz, since

its manufacturing in 2019. Long before that, to expedite the research study of the instrument, the RLS ExoMars simulator was built in the associate unit UVa-CSIC-CAB facilities in Boecillo, Valladolid. This simulator is the base of this bachelor end-of-degree project.

So, as it can be seen, the RLS instrument is fundamental for the potential success of the entire ExoMars mission, due to the number of capabilities and possibilities of the instrument. Not for nothing, the RLS instrument was selected among a large pool of available instrument candidates for its inclusion into the ESA rover.

2.3   SPDS system on the ExoMars rover

The SPDS stands for "Sample Preparation and Distribution System" and is one among the most critical subsystems of the Rosalind Franklin rover. This system is fundamental to distribute the samples between the different instruments of the Analytical Laboratory Drawer (ALD), as these are in fixed positions. The reason behind this design is to allow the different instruments to analyse the same sample, in the same exact spots, favouring a real collaborative science between the instruments. This procedure will be carried out for the first time in other planet and will be a key feature to avoid false positives, since several instruments will confirm -or refute- the results obtained by the others. This is key for the ambitious ExoMars mission, where the final objective is the detection and identification of traces of life, always a controversial issue.

The SPDS system will crush the sample extracted by the drill, obtaining a powder with a median grain distribution of 200-250 microns that will be deposited into a refillable sample container in a rotating carrousel depicted in Figure 7 (*ESA - Robotic Exploration of Mars - Mars Sample Return*, n.d.). By rotating the carrousel, the SPDS flattening system will then flatten the surface of the sample, and then present it to the different instruments in the ALD for analysis (*ESA - Robotic Exploration of Mars - Mars Sample Return*, n.d.).

After completing the analysis, the information from the refillable container sample will be studied on Ground, and a decision will be made regarding the

expense of one of the one-use MOMA ovens placed on the carrousel for more detailed analysis of the samples (looking for minor traces of organics). Finally, the refillable container will be emptied and cleaned, to dose a new sample when available.
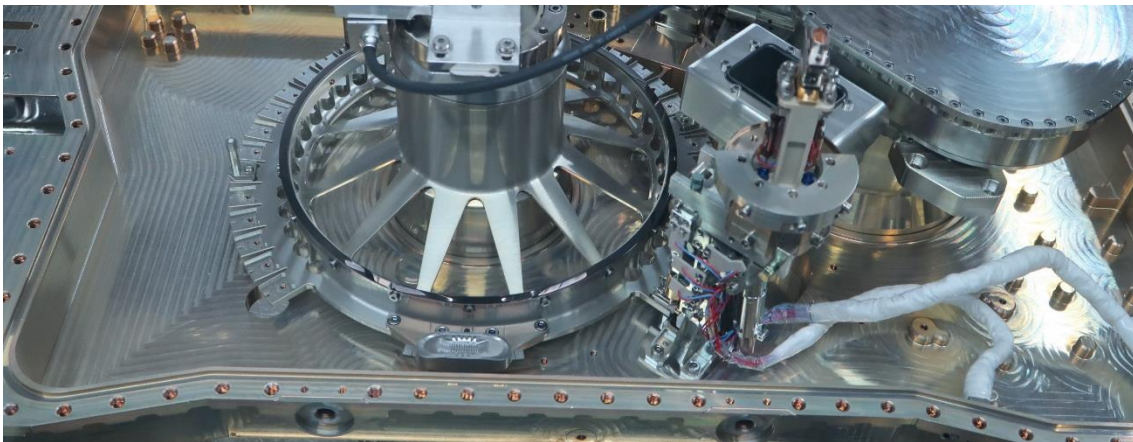
Figure 7. Flight Model of the carrousel and sample distribution system of the Rosalind Franklin Analytical Laboratory Drawer.

Integrated into the SPDS system, the rover counts with a refillable container (RC). The container will move along the carrousel surface until it reaches the flattening device to homogenize the sample and then it will be directed towards the ADL mobile laboratory. The design and form of the container are adapted to the flattening blade of the flattening mechanism, preventing particles of the powder sample from overtaking the container and obstructing the carrousel, what would hinder future operations.

As part of the ExoMars mission, to allow simultaneous sample analyses, an adapter will be mounted on top of the current refillable container. This adaptor is still under development, but an initial prototype of the idea is depicted in Figure 8.
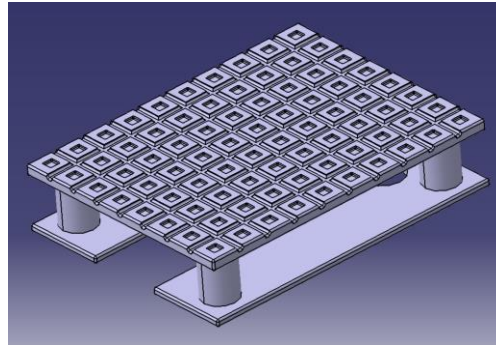
Figure 8. Multiple sample container prototype.

2.4   The RLS ExoMars Simulator

The system named RLS ExoMars Simulator is a laboratory emulator consisting of several interconnected hardware and software modules created ad hoc by the researchers of the Associated Unit UVa-CSIC-CAB of the University of Valladolid.

This system started its development in 2010, and in its current state (see Figure 9), it executes the acquisition procedures and algorithms (autofocus, fluorescence detection and removal, cosmic ray filtering, adjustment optimization of the acquisition parameters) of the RLS instrument. These were developed in the simulator and later programmed in the onboard software of the RLS instrument. But the simulator also emulates the SPDS carrousel by introducing mechanisms to position the samples under the Raman instrument optical head for analysis, as well as featuring a flattening mechanism that will be explained below.

With all these performances, the RLS ExoMars simulator allows researchers to perform automated analysis resembling the multi-point analysis performed inside the ExoMars rover. To this effect, the software was designed to allow the definition by laboratory technicians (without the need for programming skills) of complex activity plans that use the automatic mode of the instrument, while also has allowed performing combined tests with other instruments such as MicrOmega.

The RLS ExoMars Simulator thus allows faster progressing by testing the principal features of the instrument, running routine performance studies, assessing the operation of the RLS instrument or producing scientific content of interest. The RLS instrument simulator has provided the possibility to perform appraisals that would help identify the range of experiments that could be carried out within the framework of Mars exploration. With this simulator, researchers are trying to maximize the scientific return of the resulting products from the operation of the instrument on Mars *(Lopez-Reyes & Rull, 2015).*

The work performed with the simulator can be addressed from several perspectives:

1. Support the development of the RLS instrument: definition and development of the acquisition routines and algorithms of the instrument

2. Understanding of the analytical capabilities of RLS in the ExoMars rover to help defining the operational interface with the carrousel and rover: the scientific analysis of powdered samples in a multi-point fashion enabled the obtention of data and relevant information to the definition of the onboard operation mode.

3. Preparation for the mission: Investigations on samples relevant to the landing site of the mission (Oxia Planum) are performed jointly with select analysis performed using the RLS FS model (spare replica of the RLS FM model), to evaluate the detection capabilities by the instrument with the expected sample types. In addition, by analysing synthetic samples with known proportions, the simulator data help to create calibration curves that will allow the quantification of mineral abundances in mixtures detected by the instrument once on Mars.

4. Support during Martian operations: The simulator will play a key role together with the Ground Test Model (GTM) -a replica of the rover- and the RLS FS in the support needed during the operations on Mars. The simulator will be used during this time for scientific support (analysing

samples or replicating analysis) which may help interpret and understand the data gathered from RLS.

Considering all this, it is rather obvious that one of the main objectives of the simulator is to emulate the RLS instrument as realistically as possible. It is in this framework where this work is developed. Parts 3 and 4 of this manuscript cover the works performed to integrate, test and evaluate the performance of the simulator in its current configuration in comparison with the new one (the RAD1), and also with the RLS FS available data.

2.4.1 Hardware

To cover all these functionalities, the simulator counts with several hardware parts such as cameras, lights, laser, spectrometer, positioners and flattening system. Each part of the simulator is designed to replicate accordingly the behaviour of different parts of the real RLS instrument and the SPDS system. For instance, the spectrometer, as one of the most important hardware components, is expected to replicate the technical characteristics of the RLS instrument precisely. In this context, the available CompassT spectrometer offered some limitations that are expected to be fulfilled with the inclusion of the RAD1 spectrometer in the present project. Other hardware components, such as the lights, are intended exclusively for improving the interaction between the operator and the hardware. These LED cameras are only present in the ExoMars simulator and are not a constituent part of the real RLS instrument. At the same time, the presence of cameras is understood in the necessity of identifying clear spots on minerals to proceed with the spectra acquisition later. Both cameras offer different resolutions and zooms (named 50x and 10x) and are intended for different phases of sample characterization. In their correspondent section, an in-depth explanation is provided. Finally, the laser is vital for the spectra acquisition. The simulator laser operates at a wavelength of 532 nm. Thus, a calibration to centre the laser emission to position 0 with the spectrometer in use is required, in order to obtain valid data and detect the presence of certain materials and chemical compounds at their specific Raman deviation. While the laser is off, the spectrometer can only obtain dark spectra (valuable for noise extraction). As for

the flattening mechanism and the positioners, both are hardware components responsible for imitating the carrousel movement, part of the SPDS system. The positioners control three axis, namely X, Y and Z, which are responsible for lateral movement of the sample and, at the same time, height up/down positioning of the optical head transmitter. The simulator and its constituent parts are illustrated in Figure 9.
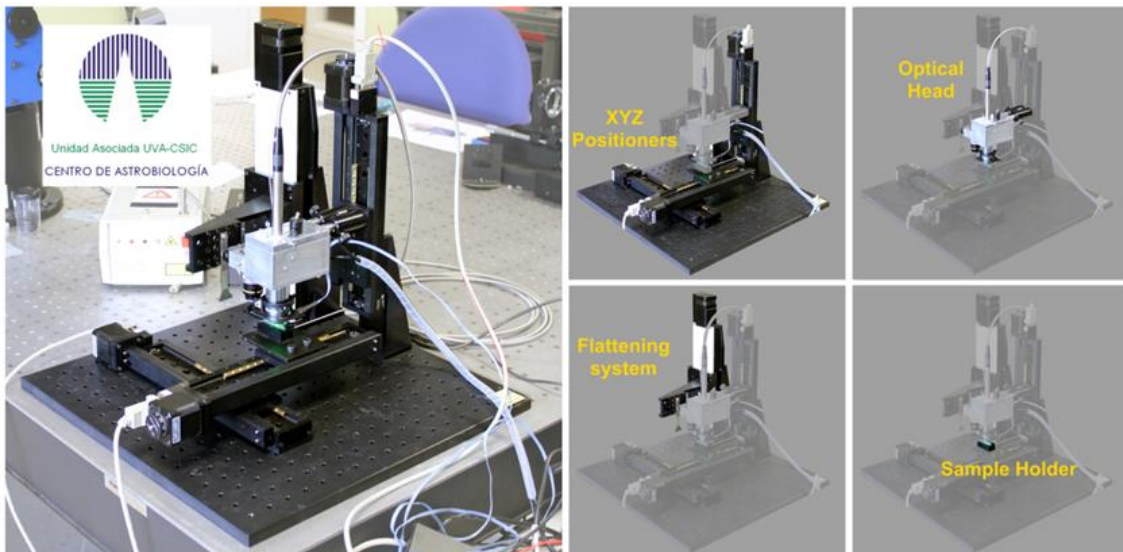
Figure 9. RLS ExoMars Simulator.

2.4.1.1 Positioners

The basic configuration of the simulator consists of an XYZ position system *(Lopez-Reyes & Rull, 2015)*. The Z axis controls the distance of the optical head in respect of the sample position. On the other hand, X and Y axis control the movement of the sample in different lateral directions to direct the sample until it reaches the desirable position. The positioners are the hardware introduced to emulate the operation mode of the SPDS system, concretely, the carrousel. The circular line traced by the carrousel on the samples can be emulated using the X-Y positioning system. The spatial resolution of the system is 2.5 microns, with a travel range of ~20 cm. The positioners integrated with the rest of components of the simulator are shown in Figure 10. The

Universidad de **Valladolid**

XYZ positioners are fabricated by Standa (Model 8MT175-200, with a specific range of 20 cm for the XY postioners and 8MT175-150 Model for the Z axis with a range of 15 cm). The microcontrollers implemented are Standa 8SMC1-USBhF, powered with 12V and including a 1.5A Microstep Driver.
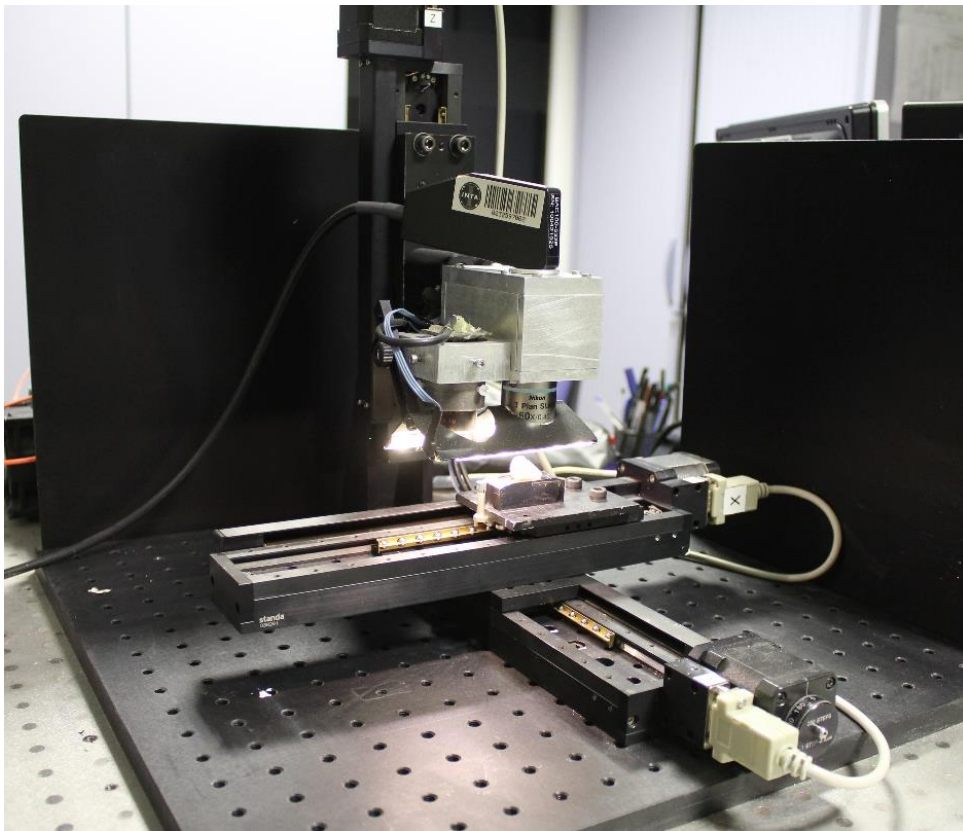
Figure 10. General view of the simulator, X, Y and Z positioners are insight.

2.4.1.2 Spectrometer

The spectrometer constitutes the domain where this project is focused. So far, a commercial CompassT spectrometer had been implemented into the simulator. The results obtained with it were limited, due to important differences with the real RLS spectrometer. Figure 11 shows the laser (light) together with the CompassT spectrometer on top (dark).

Figure 11. CompassT Spectrometer (dark colored) on top of the laser box (light colored).

2.4.1.3 Laser

The laser (Figure 11) is a commercial BWTEK continuous green laser at 532 nm, 100 mW power, connected with a USB cable to the computer. The power can be regulated in percentage and can be either commanded manually or programmatically from the computer.

2.4.1.4 Cameras

The Simulator implements two cameras with different resolution and characteristics that can be positioned over the samples to improve its study. The first objective is a Nikon 10X/0.25 Pol, WD 7.0, only used for imaging purposes and providing a field of view of 1600 x 1200 squared microns. The idea of this first objective is to imitate the MicrOmega instrument. The second lent used is a Nikon L Plan SLWD 50X/0.45 EPI, WD 13 mm, which provides a field of view of 280 x 210 square microns. This second camera is intended for imaging and also for better positioning of the Raman laser, allowing a confocal configuration, which permits the detection of what part of the sample the laser is hitting *(Lopez-Reyes & Rull, 2015)*.

2.4.1.5 Lights

Lights included in the ExoMars simulator are positioned in the optical head adaptor and moved using the Z axis positioners. The purpose of these lights is to assure, together with the use of the cameras, that a clear and smooth area of a sample is chosen for analysis. A capture of the lights during standard operation is depicted in Figure 12.

The simulator includes two LED lights connected to a COM port with an identifier from 0 to 30. This number depends on the USB connector that has been used. As part of the software, a checking control of all the ports is performed. The code starts checking the COM0 port, then COM1, COM2, ... until a connection on the port is detected. If the control reaches the 30th position without finding a connection, an error message is displayed to the user. Each COM port is connected to a specific electronic board, controlled by a USB-series converter.
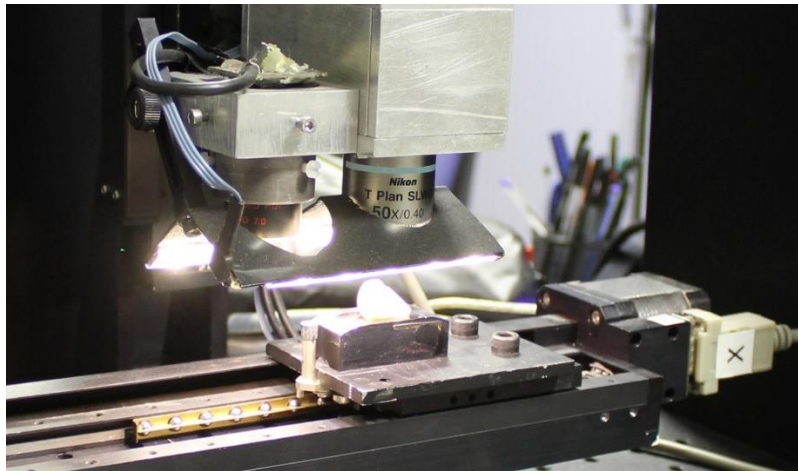
Figure 12. Lights operating on a sample.

2.4.1.6 Flattening mechanism

Another key functionality of the Simulator is the flattening sample mechanism. In the simulator, the sample powder is flattened using a rover-like system and, together with the positioning system (system in charge of moving the sample until it reaches the instrument optical head) will emulate the SPDS system. At this point, is crucial to highlight that in the current configuration of the Simulator, the flattening mechanism is not operating. Thus, analysis directly over the raw samples are performed. As for this project, the results that will be studied are based on solid minerals, which is why no flattening system is required.
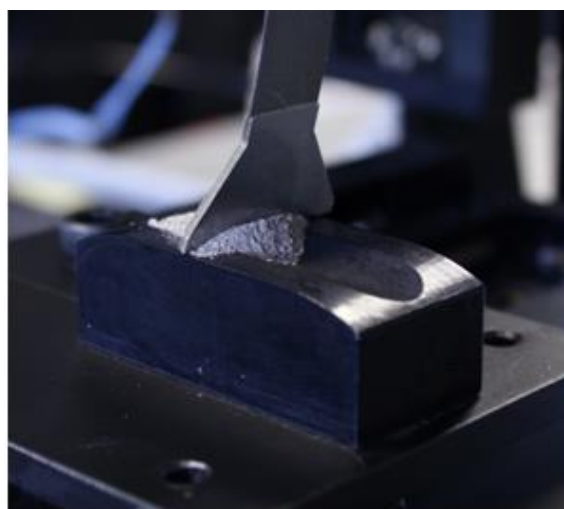
Figure 13. Flattening blade actuating on a sample.

2.4.1.7 Sample container

The refillable container included in the ExoMars simulator is attached to the XY positioners and it is an exact replica of the RC container mounted on the rover. A picture of the container is shown in Figure 14.
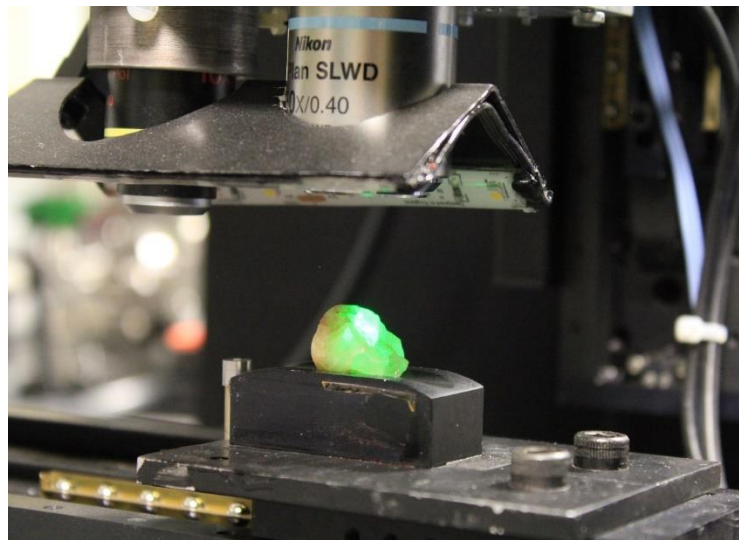
Figure 14. Refillable container of the simulator with a mineral under analysis.

2.4.2 Software

2.4.2.1 Operation modes

The Simulator is programmed to enable two different types of operation: Manual mode and automatic mode. A small insight into how the manual capture and the automatic process work are presented here.

2.4.2.1.1 Manual Operation

The manual operation offers researchers the possibility to control small experiments. This manual operation is conceived as a helpful tool for the automatic mode, enabling the right positioning of a sample or making sure the

experiments would be successful by acquiring an initial spectrum with the configuration details settled, such as the acquisition time. Making sure that non-desirable effects appear or the presence of troublesome spikes is minimal**.** A common manual operation of the simulator works as follows:

1. **Sample preparation using Cameras and Positioners:** X and Y axis provide movement to place the sample under the optical head, while the Z axis permits an up/down displacement of the sample. Led lights can be switched on in this phase to improve the visibility of the operator. The idea is to obtain a clear, non-distorted version of the sample on the camera. The autofocus function (described in section 2.4.2.1.2) can also be used.

2. **Laser:** As soon as the sample is well-positioned, lights are turned off and the laser power is directed towards the material under analysis. The simulator enables operation at 100% of the power capacity of the laser, although the RLS instrument works at a maximum of around 30%, to ensure sample safety.

3. **Spectra Acquisition.** At this point, the experiment is ready to begin. Scan or continuous scan buttons are available to capture the spectrum. Further controls under the visualization window allow the visualization of the spectra in different units. As part of the capture process and, in order to minimize the noise, a dark scan (scan with no laser power) can be obtained and subtracted from the spectrum.

2.4.2.1.2   Automatic operation

The automatic operation mode in the ExoMars simulator operates in two different ways: the automatic mode or the activity plan. The activity plan is a much more complex mode designed to encapsulate the operation of the automatic mode in further software improvements.

The need for an automatic mode is based in the necessity of performing similar operations to the ones of the real RLS instrument. The RLS device, under

its normal operation, will acquire 20 to 39 spectra along a line of a certain sample, autofocusing and autoadjusting the acquisition parameters at each point to adapt the system to the characteristics of each point under analysis. The acquisition time is limited to 5 minutes per point.

As for the activity plan, it includes algorithms to make decisions automatically in order to obtain better data, including an autofocus image analysis based on the grey level variance of a region of the image, making latter decisions to modify or maintain the focusing level.

2.4.2.1.3 Configuration parameters

Before commencing a Scan operation (manual or automatic) it is important to consider the different variables. The following variables are key to enable the right operation of the simulator:

- Integration time:

The integration time is the time during which the spectrometer CCD is capturing photons from the collection fiber of the spectrometer *(Lopez-Reyes & Rull, 2015)*. The RLS will check if the reference spectra is saturated. If so, a shorter integration time will be set to ensure the right operation of the rest of the instrument *(Lopez-Reyes & Rull, 2015)*.

- Accumulations:

This parameter defines the number of acquisitions to be averaged with the same integration time. The higher the number of spectra accumulated, the better the quality of the final spectrum, drastically improving the obtained SNR.

2.4.2.2 Software integrity

The ExoMars Simulator software controls all the described hardware components: Laser, positioners, spectrometer, lights and cameras. These constitutive parts are controlled by a custom-built LabVIEW software. The decision of using this programming language is justified by the necessity of facilitating further integration with other systems. At the same time, LabVIEW provides a better graphical interface and a better control of the multiple USB ports needed for the management of the hardware components. A previous software with C++ was available, but issues with the integration of other parts resulted in the discontinuation of this line of work and the current LabVIEW software was developed instead.

The code is structured in each part with a Stacked Sequence Structure of LabVIEW. Generally, a first initialization window exists, as well as another one with the main code and finally, an additional tab to execute the end of the code that was running.

The user interface is the Labview Front Panel of the main .VI file. It consists of two pages: Page 1 and Page 2, as shown in Figure 15 and Figure 16.
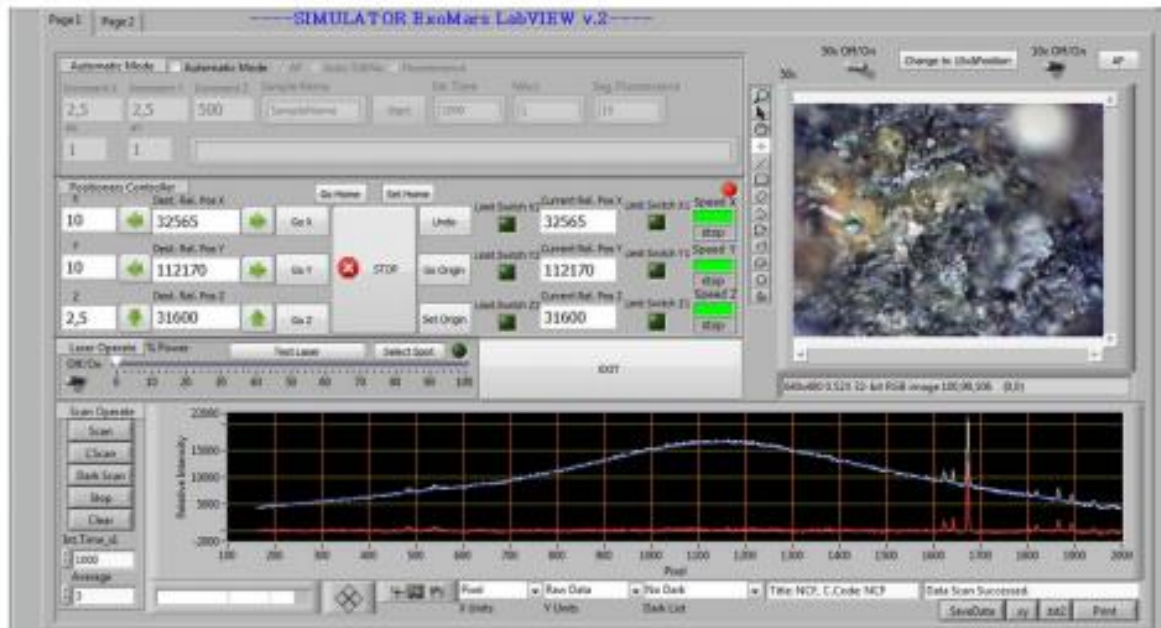
Figure 15. Labview front panel page 1 of the ExoMars Simulator.

Page 1 controls the manual operation of the system. However, the automatic control mode is also present at the top of the interface. The cameras control is located on the right side. The Positioners control is situated in the centre, together with the laser control. The scan processing tools and buttons, and the spectra visualization graph are placed at the bottom of the interface.

There are different kinds of scan modes with the simulator. On the one hand, a unique spectrum capture can be obtained by pressing the Scan button and setting the right Integration time and Average value (accumulation number). On the other hand, the system allows also a continuous acquisition, by pressing the CScan button. A dark scan is also possible to perform. This Scan is similar to a normal Scan, but without laser light. This Dark Scan is intended to mitigate the effect of external light noise. The Dark is subtracted to the scan capture obtained with the laser to reduce the non-desirable effects related to ambient light or non-random noise (e.g. hot or cold pixels on the CCD).

At the bottom of the graph, different units such as Raman shift, Wavelength, Pixels o Wavenumber can be selected to visualize the spectral data in different units.

The Activity Plan graphic interface is located in Page 2. The Activity Plan is a powerful tool that allows scientific personnel to program activities without further interaction with the system by a set of pre-programmed code functions, reducing the amount of manual tasks and enabling operation of the software during night periods, for example. This Activity Plan is presented in depth in its correspondent title of this section.
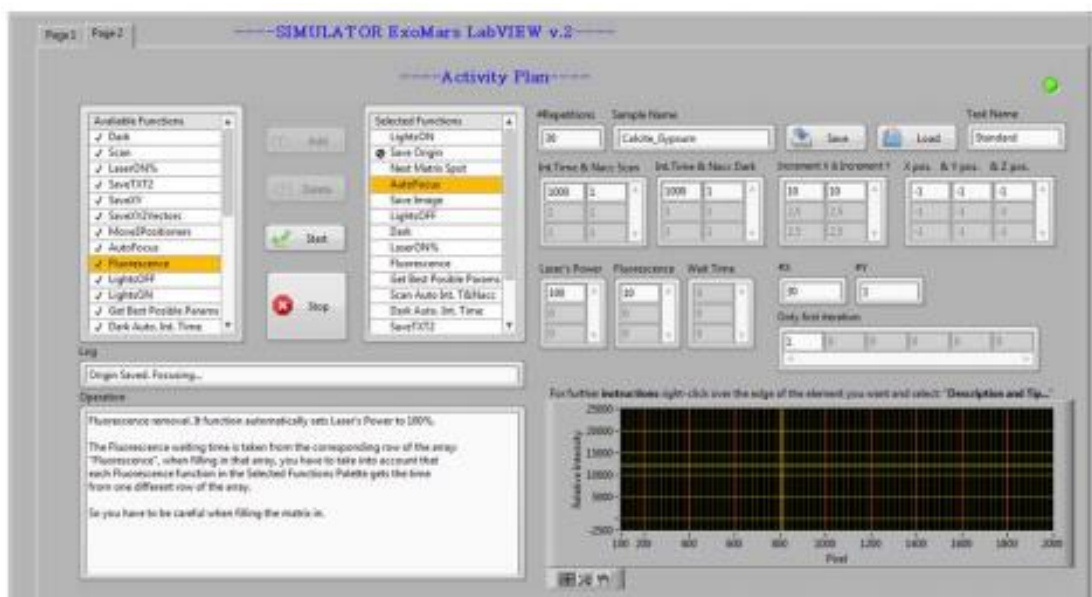
Figure 16. LabVIEW front panel page 2 of the ExoMars Simulator.

The interface has two Listboxes, which contain the available and selected functions. The text indicator *Log* provides information about the task the activity plan is carrying out at that moment and the Operation field provides information about the functionalities of each function. To administrate the functions the Add, Delete, Start and Stop buttons are used.

On the right part of the screen the controls and parameterization of the functions are located, allowing the control of the number of repetitions of the activity, integration time, number of accumulations, etc. At the same

time, the name of the activity can be detailed in the *Sample Name* area and saved wherever the user selects. This software also allows saving and retrieving activity plans.

2.5 RAD1 Spectrometer

The constant effort of the ERICA group has always been directed towards achieving a much more realistic simulator of the RLS instrument. For this reason, the RAD1 spectrometer (Figure 17) was created. The work performed in this project for the integration of the RAD1 device into the RLS ExoMars Simulator is a step forward into improving its capabilities, as it will allow laboratory experiments to assess and validate more accurately the performance of the real flight instrument.

2.5.1 Hardware

RAD1 is an acronym for RAman Demostrator 1. This device is a laboratory spectrometer (not intended for flight) that has the same design as the RLS instrument. i.e., it was built in order to imitate the technical characteristics of the RLS instrument spectrometer (see *Table 1*), without the burden imposed by the qualification for a space environment. The RAD1 model counts with the same optical design as RLS, developed through the use of commercial optics, but resulting in the same magnification and optical configuration. The optics consist of a Pentax SMC 70mm f2.4 objective for collimation, and a Nikon 50mm f1.4 objective for focusing the light on the Hamamatsu CCD S10141/1109S (refrigerated at -9.5ºC, with 2068 x 512 12-microns-pixels). The diffraction grating and resulting geometry is identical to the RLS instrument spectrometer (*ESA - Robotic Exploration of Mars - Mars Sample Return*, n.d.), using a Wasatch Photonics grating of 1800 lines per mm. The input slit of the spectrometer is, by design, given by the collection fiber core diameter, which is 50 microns for the RLS instrument.
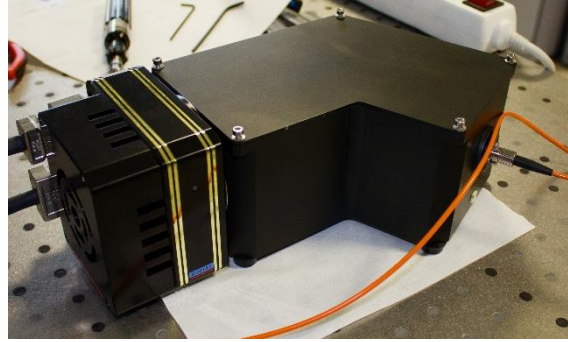
Figure 17. RAD1 spectrometer (Lopez-Reyes & Rull, 2015).

As depicted in *Table 1*, the most important characteristics, such as the optical magnification or the diffraction grating are identical. Although other characteristics differ slightly (pixel size, CCD operation temperature, CCD size, etc.), these are not critical for the functionalities of the spectrometer. RAD1 is, thus, a spectrometer with quite similar performances compared to the real RLS instrument. In section *Part 2: performance evaluation of the RLS ExoMars Simulator* of this project, the Simulator operating with the RAD1 is compared to the results of the RLS FS model.

Parameter	RLS	RAD1
CCD	Custom E2V	Hamamatsu S10141/1109S
CCD operating temperature (°C)	-10	-9.5
CCD size	2143 x 512	2068 x 512
Pixel size (μm^2)	15x15	12x12
Optical magnification	0.7	0.7
Diffraction grating	Wasacht photonics:1800 lines Input and Output angle: 32.84°	
Spectral range (nm)	537 - 667	491 - 704
Spectral range (cm^{-1})	200 to 3800	-1532 to 4606
Resolution (cm^{-1})	8 (rs < 2000 cm^{-1}) 7 (rs > 2000 cm^{-1})	12.6 (rs = 483 cm^{-1}) 8.2 (rs = 2574 cm^{-1}) 6.4 (rs = 4567 cm^{-1})

Table 1. RLS and RAD1 comparison (Lopez-Reyes & Rull, 2015).

.

Finally, in order to provide better usability of the equipment, the RAD1 demonstrator was integrated in a case with an independent laser to allow its transportation and to permit operation in external sites using portable batteries. An image of the case is displayed in Figure 18.

Figure 18. RAD1 spectrometer, portable version.

2.5.2 Software

The LabVIEW software of the Hamamatsu commercial spectrometer was custom-developed to control the RAD1 spectrometer. This code is structured following a sequential programming method. The software starts by calling the initialization libraries of the Hamamatsu spectrometer. Secondly, the code checks the temperature of the CCD continuously using a While loop. Finally, an event structure is presented. This event structure controls the capture process of the RAD1 by calling subsequent .VIs containing the principal libraries of the capture process.

The interface is shown in Figure 19. It contains the main controls that can be used. As it can be observed, most of the screen is occupied by the LabVIEW Graph. This graph displays the Raman spectra captured by the instrument. The X-axis indicates the wavenumber in cm^{-1}, whereas the Y-axis shows the intensity received. In this spectrum, we expect to register a peak in 0 cm^{-1} that would indicate that the laser is well calibrated.
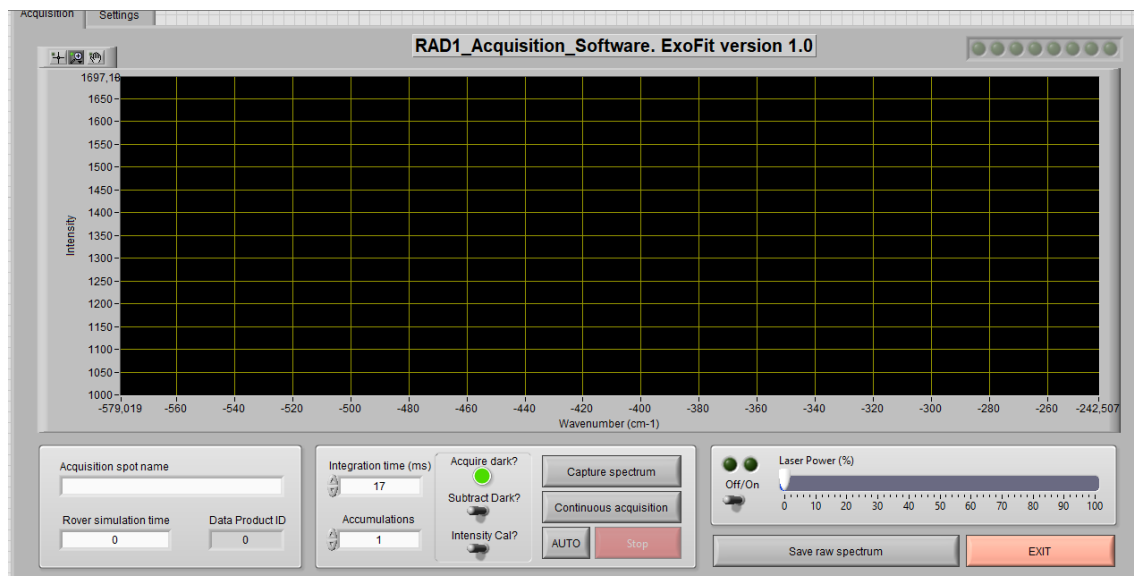
Figure 19. RAD1 software interface.

3 Part 1: Integration of the RAD1 spectrometer in the RLS ExoMars Simulator

As stated in section 2.4, the development of the RLS ExoMars Simulator is fundamental to establish a clear work path for researchers of the Associate Unit UVa-CSIC-CAB, in terms of scientific return of the ExoMars mission. The scientific outcome of this simulator is promising for several reasons. Firstly, it has supposed the beginning of a good set of scientific publications. Data extracted from the simulator has been carefully studied and the experiments ran have allowed researchers to identify key possibilities of the actual RLS instrument and has also been key during the development of the instrument. The RLS simulator includes the capability of performing not only manual operations, but also the possibility to carry out automatic spectra acquisition through a set of algorithms developed ad-hoc for the RLS instrument. The simulator was used to define the algorithms of the RLS instrument and can now be utilized to replicate the same operation mode of the RLS instrument. At the same time, the SPDS system has been emulated with three positioners and a sample flattening mechanical device. Therefore, for the reasons explained, the simulator has been a success and the effort of the group has been focused into introducing further improvements that will lead to more precise data analysis and characterization.

The foundational objective of the simulator was to replicate as precisely as possible the operation run under the real RLS instrument. In this line, the work presented in sections *Part 1: Integration of the RAD1 spectrometer in the RLS ExoMars Simulator* and *Part 2: performance evaluation of the RLS ExoMars Simulator will potentially* contribute to the general improvement of the simulator by integrating the software of the RAD1 spectrometer. Hence, a general overall improvement of spectra acquisition is expected, as well as a better representativity of the RLS instrument, since the RAD1 spectrometer characteristics are closer to the characteristics of the real spectrometer mounted on the rover. After this work, the RLS ExoMars Simulator will be able to work in

two different configurations, letting the user select the working spectrometer for the analysis.

The project development was affected drastically by the global Corona Crisis. For this reason, an entry (*Corona Crisis work*) was introduced to explain in detail the necessities required for the success of the present end-of-studies project.

3.1   Corona Crisis work scheme

Due to the Corona Crisis (deriving in a worldwide pandemic), suffered while developing the present end-of-studies project, an appropriate approach was required in order to complete this work. Firstly, a remote operation structure was needed to ensure the security of people involved and, at the same time, comply with the new rules implemented by the University of Valladolid and derived from the State of Alarm decreed in the Spanish territory by the competent authorities. Hence, all the communication maintained during the project was remote using different tools available for this purpose, including videocalls and settling a remote computer scheme (counting also with a remote control of the simulator), RAD1 control, two laptops, and power supply remote control (to ensure hardware safety and also to allow restarting the instruments remotely).

The development of the software code required, was implemented establishing a TeamViewer session to control the GPC laptop where the RAD1 spectrometer was controlled from. The simulator code was downloaded in this computer (using a code repository with subversion) and modified by isolating the software parts that required access to hardware (except the RAD1 spectrometer). The version control was kept with the subversion repository at all times, ensuring that the Simulator was able to work in the usual analysis from the laboratory, thus minimizing the impact on the normal activities of the laboratory. All the hardware and computers remained in the Associate Unit UVa-CSIC-CAB facilities in Boecillo. In the second phase of the project, the code needed testing and validation. For this reason, a second remote communication was established. This new communication was established using the Remote Desktop

Connection, connecting the GPC computer to the Simulator Computer Controller. This computer has the master control of the hardware parts of the simulator. As for the works of the present project requiring an in-situ manipulation (e.g. to places and analyse the samples with the simulator, or connect the optical fibers to the different spectrometers), the activities were delayed as much as possible until the University of Valladolid and official authorities allowed the reopening of university laboratories to students.

3.2 Adaptation of the RAD1 software for integration in the RLS ExoMars Simulator

As part of this project, the RAD1 software has been modified and adapted to operate in accordance with the simulator software. The code of the entire simulator software is organized in sections consisting on a main Event structure where the principal functionalities are stored. For this reason and, in order to adapt the RAD1 software to the code structure, a few changes have been introduced to allow a smoother integration into the Simulator code.

Previously the RAD1 software had been structured in a sequential way. The changes introduced organized the code with a unique Stacked sequence of 4 tabs. The fourth tab of the Stacked sequence contains the Event structure which handles 12 different event cases. Those cases are the following: *[0]"Capture", [1]"Continuous acquisition", [2]"EXIT", [3]"Save spectrum", [4]"Acquire dark?", [5]"Subtract Dark?", [6]"Intensity Cal?", [7]"Off/On", [8]"Laser Power (%)", [9]"Wavenumber calibration file", [10]"Intensity calibration file", [11]"AUTO".*

It can be easily noticed that, all the events correspond to a functionality that can be controlled by their respective button in the Acquisition Page of the Front Panel of LabVIEW.

Finally, it is important to indicate that the Event structure is set into a While loop. This While loop forces the system to operate continuously until the user presses the EXIT button or the *Abort Simulation* option in the LabVIEW panel is depressed.

Apart from this Event Structure, tabs 0, 1, 2 and 3 contain code to initialize the laser and the spectrometer. The .VIs used in these sections are listed here: RAD1_Initialization, RAD1_Configuration, OpenCalibrationFile, PowerSet, Create_XML_File and IntensityCalibration.

Hereafter, in Figure 20, the new code structure is displayed together with the main Event structure of the fourth tab, which contains the functionalities available for the users.
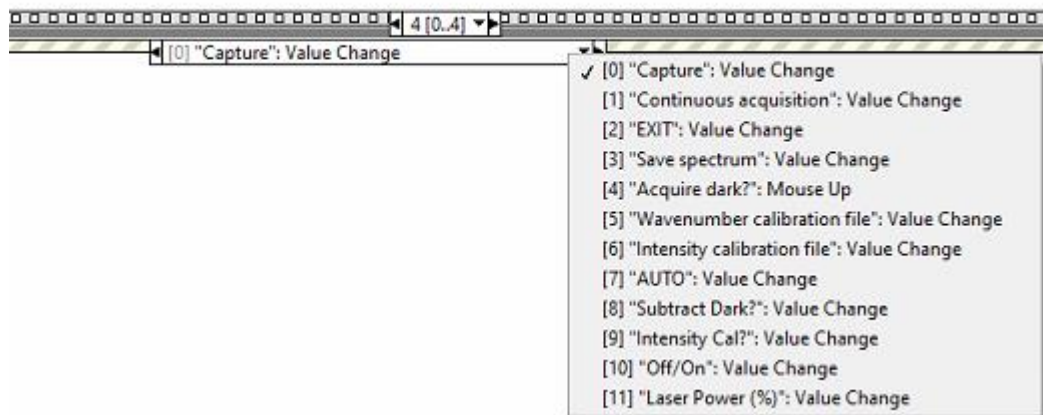
Figure 20. New RAD1 software adaptation, showing the fourth tab of the Stacked Sequence containing the 12 functionalities of the software.

To proceed with the migration phase, it was fundamental to establish an initial comparison between data treatment in the simulator regarding the spectrometer and the way spectra were captured and processed in the RAD1 software. The data acquisition philosophy of each spectrometer differed drastically in some respects and remained equal in other parts. For this reason, a mix structure was created to reuse as much code as possible, only needing to create a small set of specific new variables for the RAD1 software.

3.3 Integration of the RAD1 into the RLS ExoMars Simulator software

Once the new stacked RAD1 Software was operative and capturing correct Raman spectra, the next step in the development of this project was to migrate the software into the entire ExoMars Simulator Software. To explain the migration and integration process, the following sections put together the most substantial modifications.

3.3.1 Updating the design philosophy: making it modular and scalable

The simulator code was developed without taking into consideration future updates and changes. Consequently, it was not organized in a modular way. As part of this project, the simulator code has been adapted to make it as scalable as possible to allow the integration of the RAD1 spectrometer, but also to facilitate potential future modifications. The scalable process began by defining the variables shared by both spectrometers. The need for a new set of variables for the RAD1 was stated, so that the creation of a new RAD1 background variables control handler was required. As a result, a mix approach was performed, maintaining the previous software data treatment as immutable as possible, but introducing new variables required by the RAD1 spectrometer, since some data operations differed between spectrometers.

3.3.2 Interface redesign

A general modification of the interface was required, in order to accommodate several changes. Though very similar with respect to the previous interface, some modifications were included: a radio button to select the working spectrometer, the *Laser Wavelength* control input (it was necessary to remove the hardcoded Wavelenght constant, which did not allow manual control by the user) and a new laser power% indicator which allows the user to set a certain number with the keyboard as a complement to the power control slider.
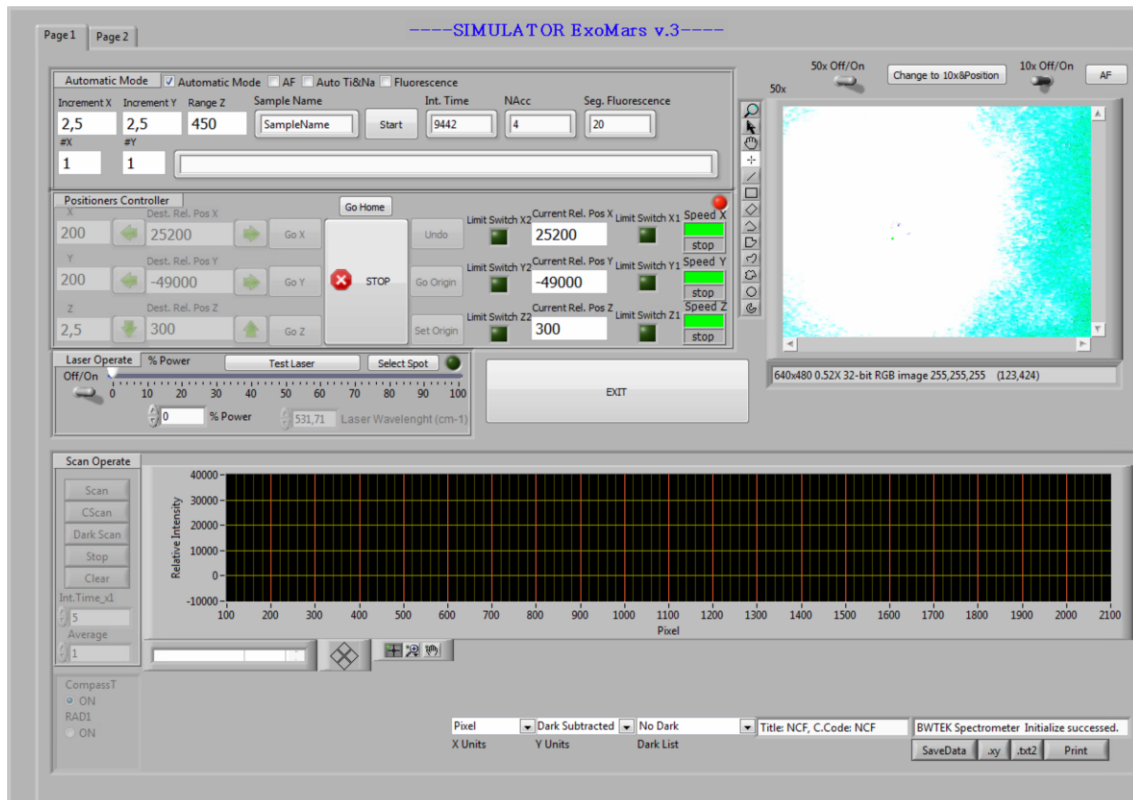
Figure 21. Simulator interface version 3, where the spectrometer and laser parts include the new modifications.

In the current configuration, the simulator is operative with two different spectrometers. For this reason, each spectrometer is selected in the user interface with a *Selection box*, as presented in Figure 21. Simulator interface version 3, where the spectrometer and laser parts include the new modifications.

3.3.3 Achieving modularity

Achieving full modularity with a strict separation between spectrometers (i.e. by having one sub-vi for each spectrometer in one part of the code only) is not something possible with this software, given the multiple interactions during the execution between the spectrometer libraries and the acquired data, and the user interface. However, all the execution points that are specific to a determined spectrometer have been identified, isolated and secured with a variable in a case

selector linked to the front panel radio buttons where the user can select the spectrometer to work with. To clarify this extreme, Figure 22 shows an example of how the code was divided according to the spectrometer in use. In Figure 22, the new *Spectrometer_ID* variable can be observed. This variable is filled when the user selects the spectrometer to be used.

Besides, all the hardcoded parameters associated with one spectrometer have been properly identified and parameterized, being now handled through the newly created variables associated with the corresponding spectrometer.
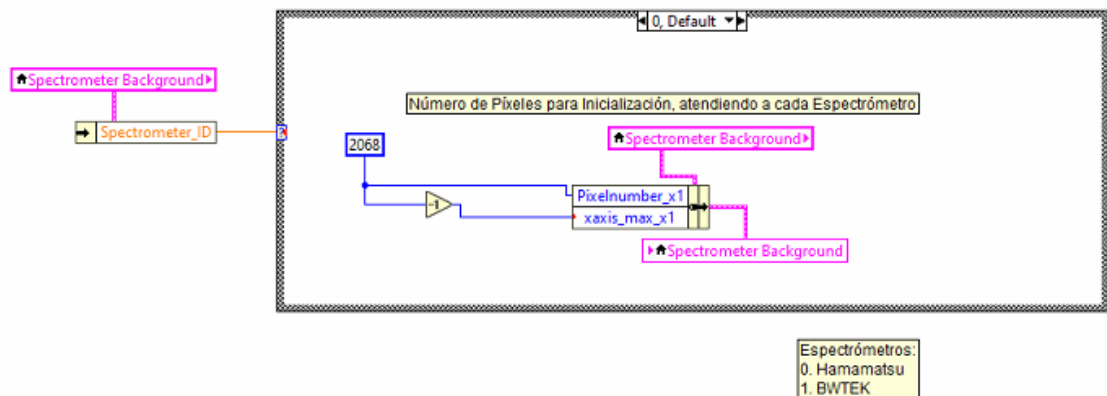
Figure 22. Case structure isolating the code of each spectrometer.

3.3.4 Scalability: common and specific variables for each spectrometer

The principal and key objective of the integration of the RAD1 into the ExoMars Simulator Software was to assure that the Simulator code structure and data processing remained immutable. To settle this initial objective, data treatment of the RAD1 software code was adapted to work efficiently within the Simulator code framework. This work is fundamental, because it will allow future scaling of the Simulator without major software modifications.

For that reason, the variables that are common to both spectrometers are loaded in the control called *Spectrometer Background control*, already present in the software to manage the CompassT spectrometer.

As previously stated, *Spectrometer Background* contains the variables used by the commercial CompassT spectrometer, which are deeply integrated into the simulator software, and are essential for a smooth performance of the simulator code. Considering this need, in this new development for the integration of the RAD1 spectrometer, all the variables in Spectrometer Control need to be filled with the RAD1 spectrometer specific values. For example, variables such as *Pixelnumber* or *Integration time* are common for both spectrometers. The rest of the variables not used in the RAD1 have been set to their default value, because they will not be used in subsequent events of execution. On the other hand, the specific data processing required by the RAD1 compared to the CompassT spectrometer, forced to create a new *Spectrometer Background Hamamatsu control*. Receiving this name, because part of the technology present in the spectrometer is built by the Hamamatsu company. These variables were needed for the initialization and configuration of the RAD1.

This way, in case further spectrometers were to be integrated in the simulator software, the same logic would be followed. All the common variables among the three spectrometers would be placed in the *Spectrometer Background control*, while the specific ones would be managed through a new dedicated *Spectrometer Background New Spectrometer control*. The spectrometer controls for the common variables and RAD1 spectrometer, with their respective variables, are presented in Figure 23.
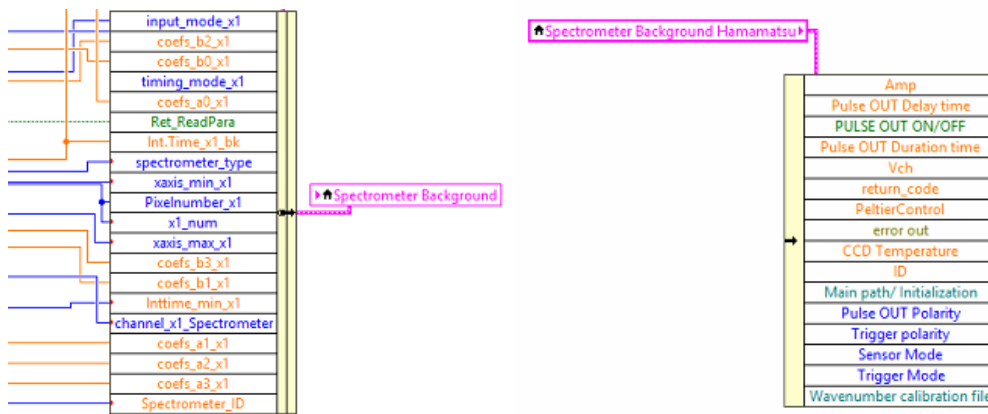
Figure 23. Common Spectrometer Background and RAD1 Spectrometer Background.

This new *Spectrometer Background Hamamatsu* control contains variables as important for the RAD1 as the Wavenumber calibration file, *Vch* (Vertical pixels) or *Hch* (Horizontal pixels), together with other variables as shown in Figure 23. Finally, a figure of the *Spectrometer Background Hamamatsu* in the interface of the programme is depicted in Figure 24.
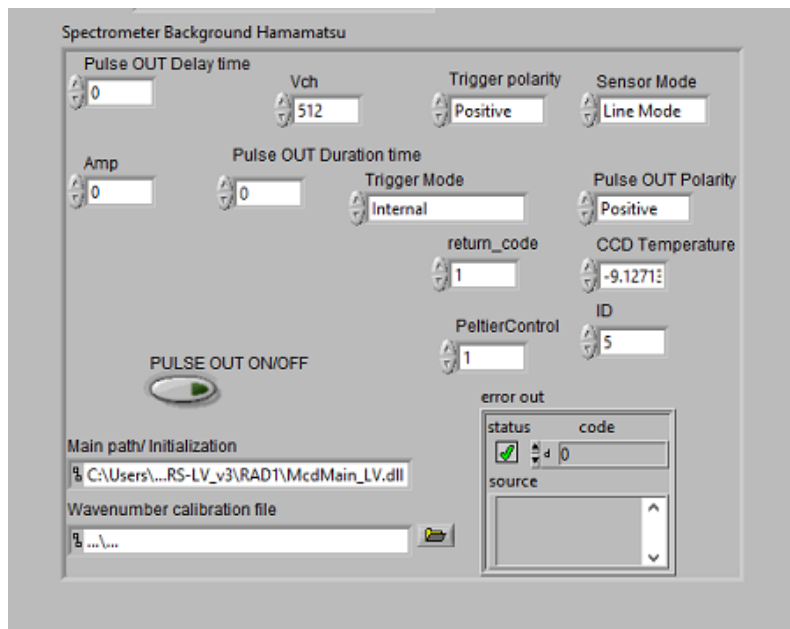
Figure 24. RAD1 spectrometer background, interface section.

Finally, due to problems with the *CaptureComplete.VI* running on automatic (thus fast) execution, some modifications were introduced to ensure a successful operation of the spectrometer. Issues related with the acquisition function *LVGetProfile* (from the RAD1 dll library) arose and some spectra returned the default 0 values. A timing issue was identified that resulted in race conditions (the spectrometer needs some time between acquisitions). Consequently, in order to sort out the malfunction, 500 ms of waiting time were introduced before the libraries *LVGetProfile* and *LVExposureTime*, guaranteeing the right operation of the spectrometer. The arrangement can be seen in Figure 25.
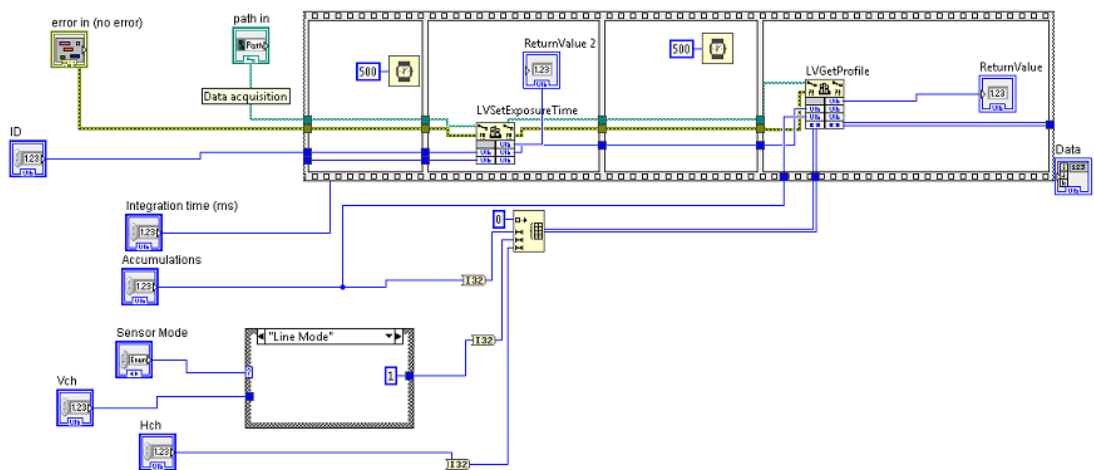
Figure 25. RAD1-Capture.vi waiting time arrangement.

3.3.5 Software control and execution flow

Once the spectrometer has been selected in the Front Panel, the code is executed. The spectrometer code is organized as follows: A general Stacked Sequence of 4 tabs controls the whole process. While the initial two tabs are responsible for the initialization of arrays, strings and numbers; the rest of the tabs contain the initialization process, together with the configuration of each spectrometer.

In order to select the spectrometer in use, a new variable called *Spectrometer_ID* was created. During each execution part, a Case Structure verifies the value of the variable *Spectrometer_ID,* which contains a number that univocally identifies the spectrometer. So far, only the RAD1 and CompassT spectrometers are included, but the new scalable design allows an easy integration of other spectrometers in the future.

In the next figures, the main Spectrometers control code will be detailed. This way, if another spectrometer was to be integrated with the simulator in the future, the critical points would be perfectly identified. The focus is going to be directed into the implemented code for the RAD1, given that no relevant modifications have been made on the CompassT control code.

-Tab 1**:**

In this first tab of the Stacked Sequence, the initialization of all the variables presence in the *Spectrometer Background* is performed. At the same time, as shown in Figure 26 , the number of pixels of a certain spectrometer is introduced in their respective variables: *Pixelnumber_x1* and *xaxis_x1*. This last variable contains one unit less than the pixel number, because the X axis goes from 0 to 2067, in the case of the RAD1 spectrometer and to 2047 in the commercial spectrometer CompassT.

Universidad de **Valladolid**
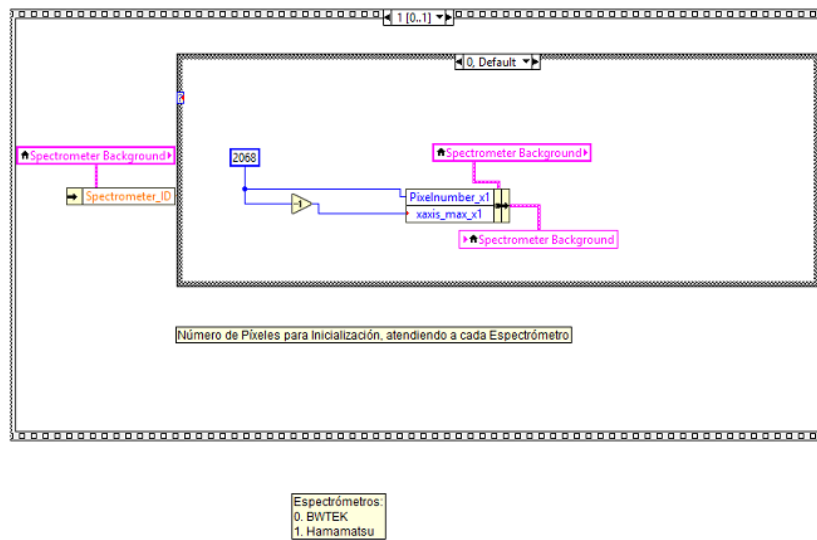
Figure 26. LabVIEW pixel selection of the RAD1 spectrometer.

On the other hand, in Figure 27 , the initialization process of the RAD1 spectrometer is performed. Notice that values not required in the case of the RAD1 have been set to their default value and will not be used during the rest of the programme (i. e. the coefficients a0, b0, b1, b2 utilized to calculate the CompassT *DataArray* for the calibration of the CompassT spectrometer).
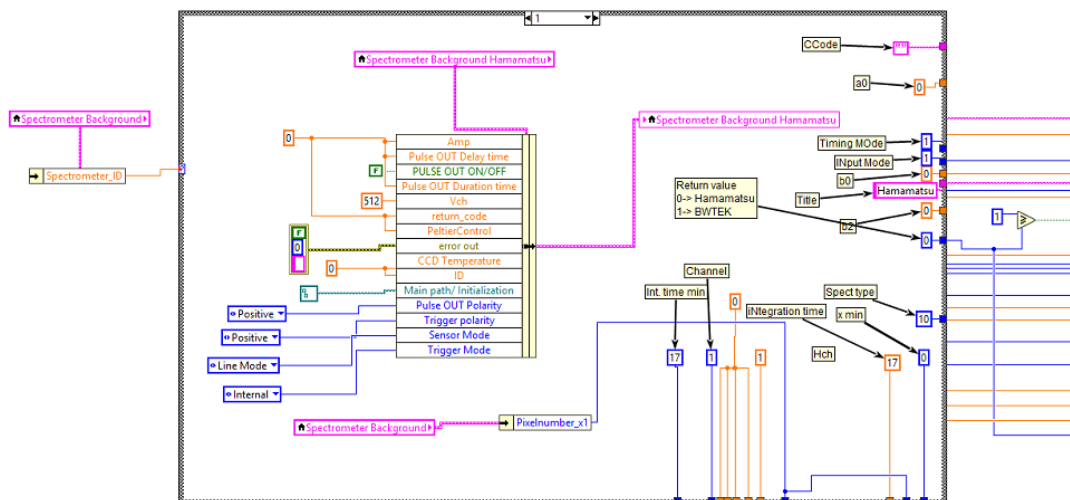
Figure 27. LabVIEW variables initialization of the RAD1 spectrometer.

Universidad de Valladolid

-Tab 2:

In the second tab, the initialization code is activated. Then, the configuration phase is called. These processes activate the spectrometer and give feedback to the user as to whether the Spectrometer is connected and running correctly.
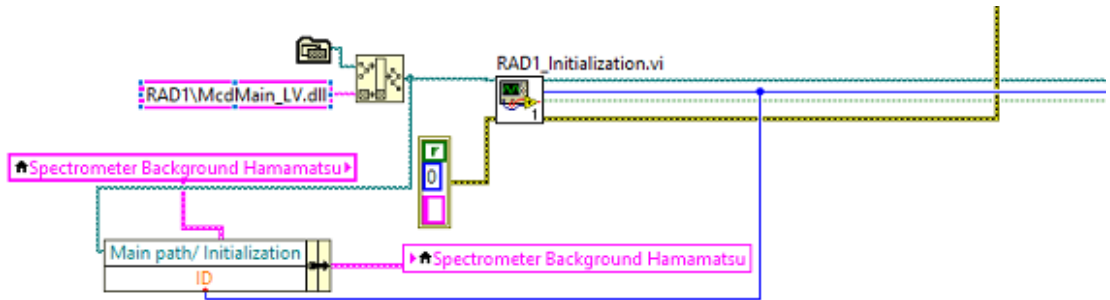
Figure 28. LabVIEW initialization of the RAD1 spectrometer.
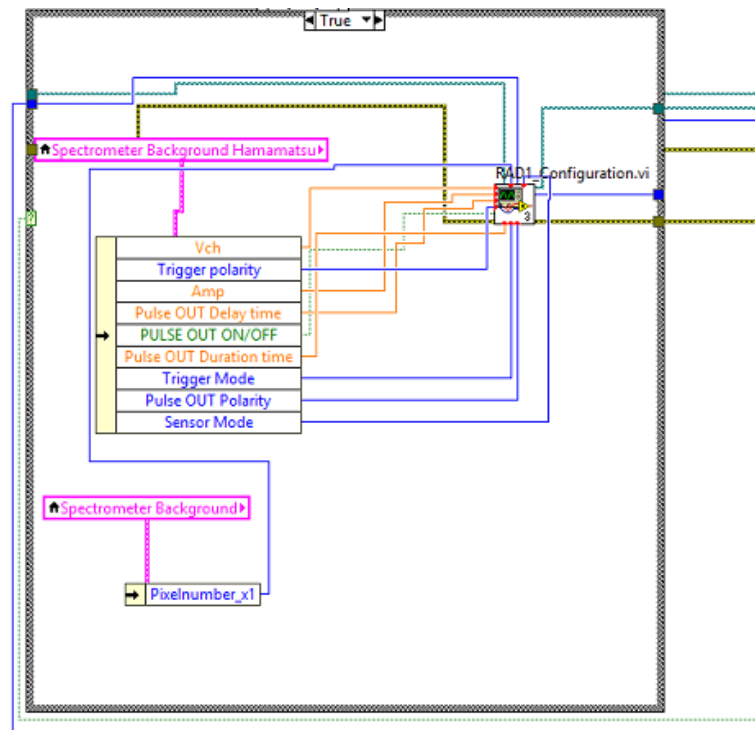
Figure 29. LabVIEW configuration call of the RAD1 spectrometer.

ETSIT

Universidad deValladolid

-Tab 3:

If the tab 2 initialization runs without any issues, the third tab is activated and the *PeltierControl*[2] library is called. The values returned from this library are stored in their correspondent variable in the *Spectrometer Background Hamamatsu*.
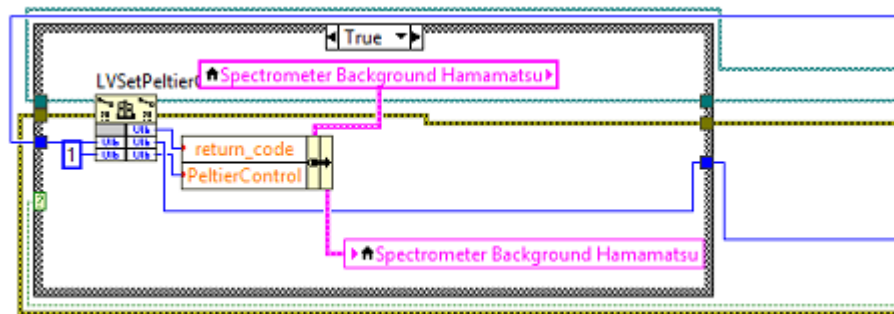
Figure 30. LabVIEW PeltierControl of the RAD1 spectrometer.

In parallel with the *PeltierControl*, the CCD temperature is checked using the *GetTemperature* library. This code, encapsulated into a While loop permits the control of the temperature at any given moment, activating or deactivating the ventilator when the temperature rises above the limit for correct operation of the RAD1 (-9.5ºC). At this point, it is important to state that both spectrometers present different temperatures ranges, which forces to have two separate temperature controls (one for each spectrometer) and that the CCD temperature is only checked once (noticed the True Boolean connected to the Conditional Terminal); due to problems during execution, which forced to take the decision of only checking it once at the beginning.

---

[2] *The Peltier is a device that regulates the temperature of the CCD. The control process of the Peltier is fundamental to allow operation of the system in the right operational temperatures. In this case, RAD1 spectrometer works in a temperature range for the CCD around -9.5 ºC (compared to the 14.5ºC of the CCD temperature of CompassT). This temperature is critical from the perspective of the thermal noise of the instrument: the lower the temperature of the CCD, the better the performance.*
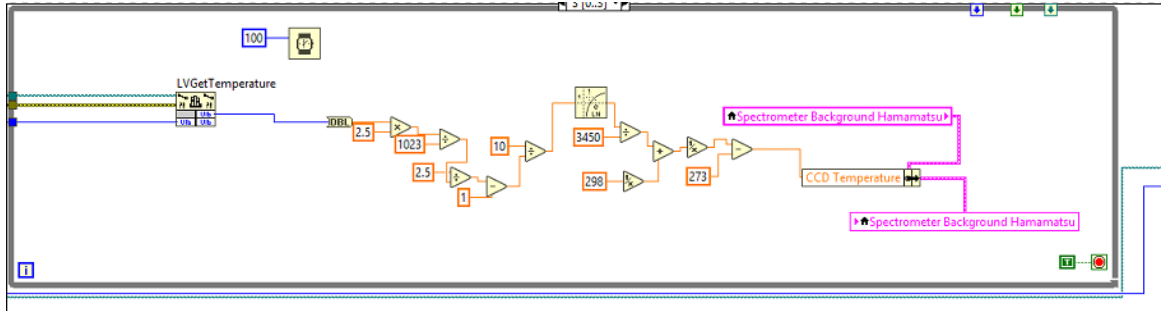
Figure 31. LabVIEW CCD Temperature control of the RAD1 spectrometer.

-Tab 4:

As soon as the previous tabs are executed, the capture tab loop waits for the user inputs. In Figure 32, the Calibration file .VI is called. This .VI of the RAD1 provides the calibration in Raman shift units. To obtain the same data in other units such as Pixels, Wavenumber or Wavelength (see section *Raman spectrometer and spectra*), several data transformation were performed and, finally, stored in the *Spectrometer Background* variables.
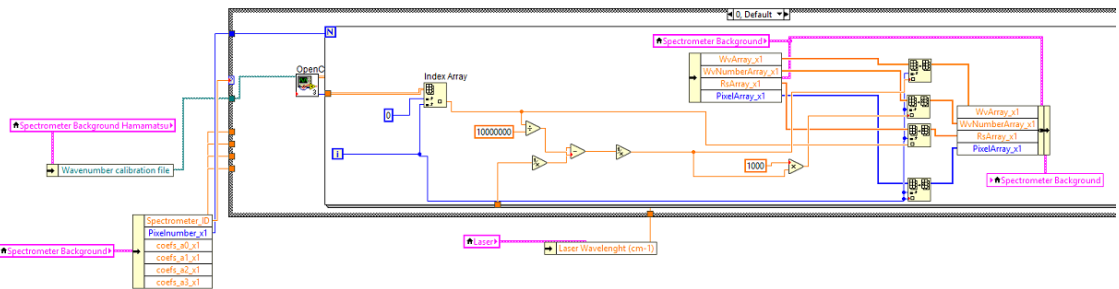
Figure 32. LabVIEW Data Units transformation of the RAD1 spectrometer.

In Figure 33 , the *RAD1-Capture.vi* is called. This .VI contains the capture process that provides the data to be shown. In order to dump the data into the variable *DataArray_x1*, a transformation was necessary in order to extract one by one each individual data number of the *Rad_Capture Array* and together with the accumulations (see section Raman spectrometer and spectra), produce the final numbers that are finally stored into the *DataArray*.
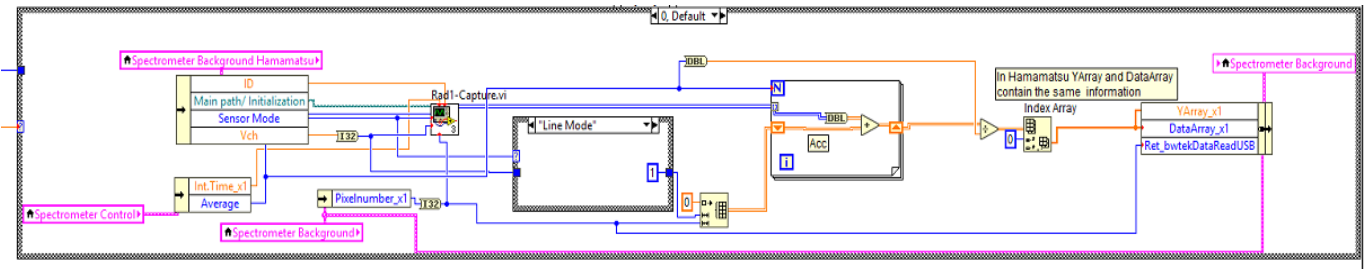
Figure 33. LabVIEW Capture process and data stored into DataArray_x1 of the RAD1 spectrometer.

3.3.6 Activity Plan: modifications.

As mentioned before, the Activity Plan is a powerful tool that enables the automatic programming of some functions, allowing activities to operate without human intervention. In this context, functions such as *Dark Manual "Int. T&Nacc", Scan Manual "Int. T&Nacc", Dark Auto. "Int. Time", Scan Auto. "Int. Time, GetBestPossibleParams and Fluorescence* have been modified to allow the operation of the RAD1 in automatic mode. These modifications are key for an effective use of the Simulator, as they represent the most critical part of the code. The Scan process is the same as presented in the previous sections. However, to comprehend in depth the implemented modifications, captures of the code are depicted here.

As the capture process is the same, the decision of creating a unique .VI to cover the entire Capture process is integrated. The sub .VI received the name of *CaptureComplete.vi.* This new sub .VI has been utilized in all the previous functions to accommodate the new capture process with the RAD1 spectrometer.
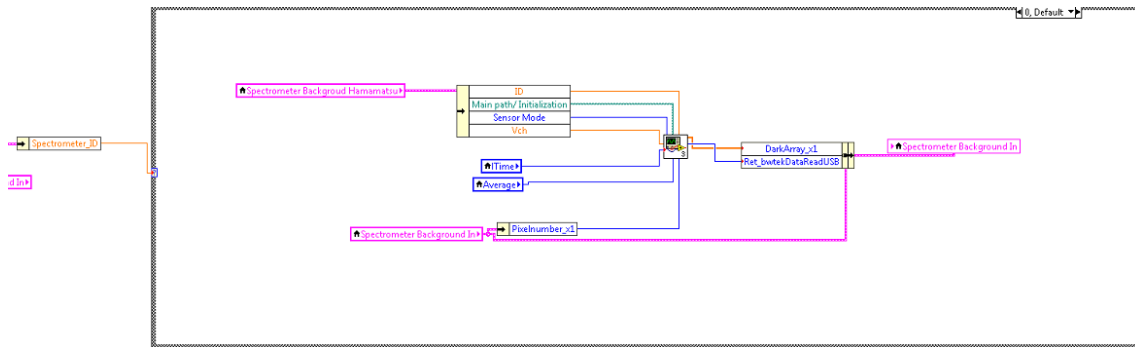
Figure 34. CaptureComplete .VI call using auxiliar Spectrometer
Background variables in Dark Manual "Int.&Nacc" function

.

Figure 34 shows the changes implemented in the *Dark Manual "Int.&Nacc"* function, but the same type of modifications have been performed in the rest of the functions where the capture takes place.

3.3.7 Ensuring a user-friendly environment

To ensure a user-friendly environment; error handlers, dynamic button enable/disable operations and information pop-ups for the user were utilized to improve the user-machine interaction. As a result, better interactivity was achieved; because code failures are not only handled internally by the software, but at the same time information is displayed to the user providing the status of the simulator. For example, Figure 35. User message, stating that the RAD1 spectrometer is not connected. shows a user message displayed when the RAD1 has been selected and the initialization process of the spectrometer fails (e.g. because it is not connected or switched on).
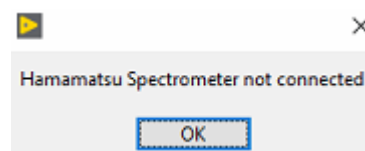
Figure 35. User message, stating that the RAD1 spectrometer is not
connected.

As a way to illustrate the user-friendly environment, Figure 36 shows the process taking place when the scan operation is performed and no issues are detected. The controls that allow the scan of the sample are set to false and a string indicating that the disconnection was a success is displayed.

Figure 36. LabVIEW disconnection phase of the RAD1 spectrometer.

3.4 Testbench, verifications and troubleshooting of the simulator

The last step of the process was to migrate the new actualization of the whole Simulator software to the computer directly connected to the actual simulator. As part of this last process, and to avoid conflicts between the versions installed in each machine, the LabVIEW software on the simulator and GPC computers was updated to the 2020 LabVIEW version: previously the simulator software was implemented using the 2013 LabVIEW version, while the new code and integration of the RAD1 software was developed in version 2014.

Test and validation acquisitions have been performed with the RAD1 spectrometer to assure a correct operation of the simulator. Initially, tests were performed manually utilizing all the functionalities available (i.e. dark scan, scan, subtract scan) and no important issues were found while executing this operation mode. However, when the Activity Plan was programmed for automatic acquisitions some problems arose. Functions such as *Scan Manual "Int. T&Nacc"* and several others (see section Activity Plan: modifications.). As part of this process, algorithms were modified when necessary to comply with the new RAD1 software proposed. A future line of work was set here, as some algorithms might need modifications in order to optimize the operation of the simulator with the RAD1 spectrometer.

Universidad de Valladolid

(This page intentionally left blank)

4 Part 2: performance evaluation of the RLS ExoMars Simulator

4.1 Introduction

Part 2 of this project is focused on the analysis of the performance of the ExoMars Simulator with the updates proposed in Part 1. At this point it is important to summarize the changes introduced in the Simulator:

The performance of the Simulator was far from close to the real operation of the RLS instrument. One of the key issues was the spectrometer in use, a commercial CompassT spectrometer with limited capabilities. For this reason, the RAD1 (RAman Demonstrator 1) was integrated into the Simulator. The main purpose is to get a performance closer to the real RLS instrument and, expectedly, results would show an important improvement in the overall performance of the Simulator in terms of acquisition quality. As it was previously described in this project, the simulator emulates the operational behaviour of the RLS real instrument. In this work, we have compared the performances of the simulator between the two available spectrometers (the commercial CompassT and the RAD1) and then compared it with the performances obtained with the RLS instrument itself. The idea behind this set of comparisons is to understand the grade of similarity achieved between the RLS FS model and the ExoMars Simulator with the new integrated RAD1 spectrometer. It is important to highlight that no data have been analysed using the RLS FM instrument -the flight model, as it is integrated in the rover. Instead, all the tests and validations have been performed using the RLS FS model -an exact replica of the RLS FM - created as part of the standard development logic of space projects, and which is used now for verification and tests on ground to prepare the RLS instrument operation on Mars.

The performance evaluation of the different spectrometers is performed by studying three different issues:

- Spectral Range: the available spectral range of the instruments is evaluated. This range is related with the optical design and cannot be modified. The rationale behind this is to understand if there are important differences between the different spectrometers.

- Spectral Resolution: This parameter is obtained by measuring the Full Width at Half Maximum (FWHM[3]) of the emission peaks. In general terms, the lower the spectral resolution, the better, given that it will be possible to better resolve adjacent or overlapping peaks. However, obtaining more narrow or wider spectral resolution would depend on the type of desired information wanted from the experiment (*What Is Spectral Resolution, and When Is It Needed? - HORIBA*, n.d.). On one hand, in order to precisely establish the chemical nature of a mineral, low/medium resolution is required. On the other hand, high spectral resolution might facilitate the identification of small changes produced in crystallinity, offering more complete information than a narrow spectral resolution, providing the possibility to detect minor changes in the shape or position of the peak.

- SNR performance and evolution with accumulations: The SNR is a well-known calculation utilized in mathematical applications to determine how good a system or process behaves with respect to noise. In this context the signal/noise ratio is a key parameter for any spectrometer (*How Do We Measure the Signal to Noise Ratio of the Raman Spectrometer?*, n.d.): the better the signal and the lower the noise, the better the spectrum clarity and quality.

---

[3] FWHM stands for Full Width at Half Maximum and can be determined as the distance between the curve points at the peak half maximum level.

The following sections describe the *Materials and Methods* used on the analysis before analysing the results from the tests in the *Results and Discussion* section. Finally, a short set of conclusions is included to wrap up this part of the work.

4.2 Materials & Methods

4.2.1 Samples

As already introduced, the aim of this work is to evaluate the performance of the RLS ExoMars Simulator in its previous configuration (with the CompassT spectrometer), with respect to the new configuration with the RAD1 spectrometer, which was, thus, used in both configurations to acquire spectra. Hence, a series of samples were analysed with the simulator.

The five minerals chosen for the experiment have been selected according to several criteria:

First, **bulk calcite** ($CaCO_3$) and **powdered diamond** were selected, as these are samples with fairly good Raman response. The analysis of these materials facilitates the characterization of the spectral resolution of the instrument, with low-time acquisitions and good SNR.

Secondly, a set of minerals present in the surface of Mars were also selected for study. These include bulk **Hematite** (FeO), abundant iron oxide that provides Mars its reddish color, **Olivine** ($(MgFe)_2SiO_4$) or **Vermiculite** ($Mg_{0.7}(Mg,Fe,Al)_6(Si,Al)_8O_{20}(OH)_4 \cdot 8H_2O$), which are selected due to their representativity of the Martian surface, concretely in Oxia Planum, landing site of the ExoMars mission.

In addition, the selection of these minerals was influenced also by the fact that they had been previously evaluated using the RLS FS model (though in powdered form), so repeating the analysis on these samples facilitated a subsequent comparison. Images of the materials (at microscopic level with a 50X objective) are shown in Figure 37, Figure 38, Figure 39, Figure 40 and Figure 41.
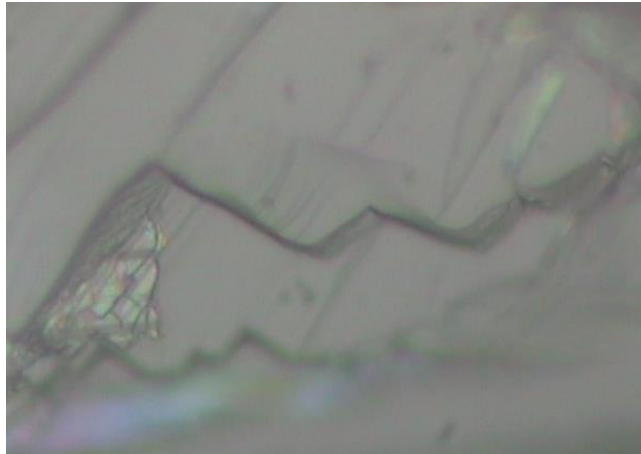
Figure 37. Calcite sample using 50X zoom microscope.
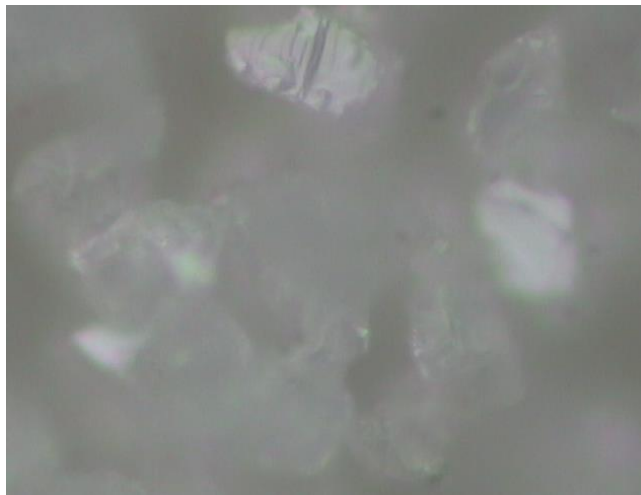
Figure 38. Powder Diamond sample using 50X zoom microscope.
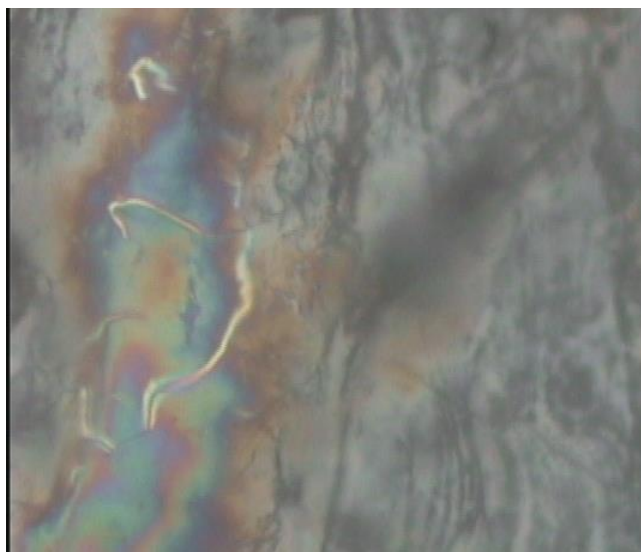
Figure 39. Vermiculite sample using 50X zoom microscope.
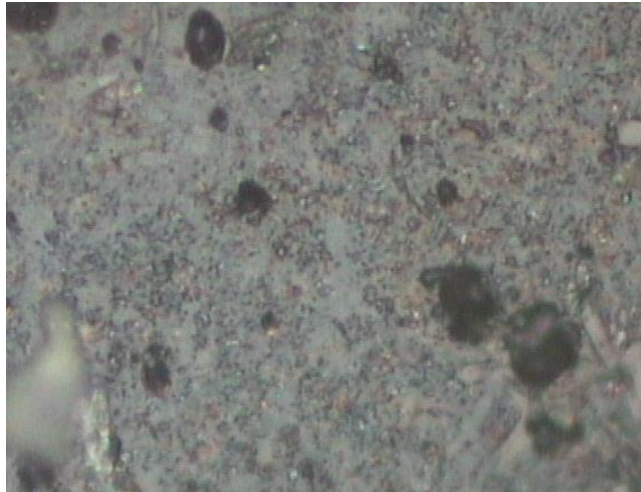
Figure 40. Olivine sample using 50X zoom microscope.
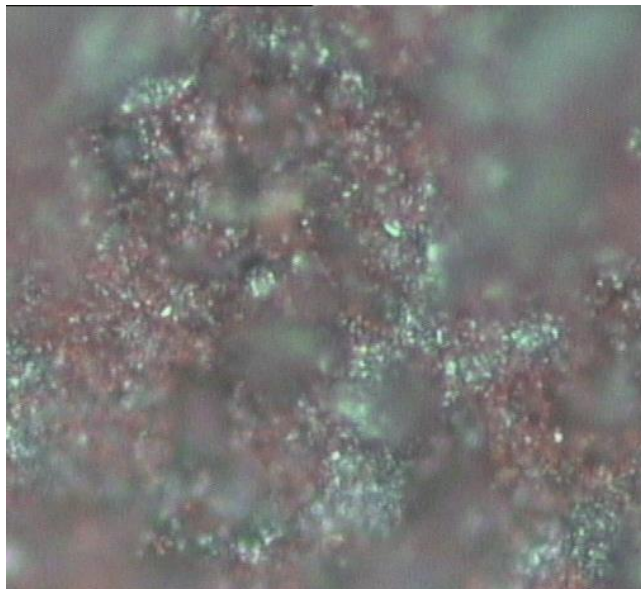
Figure 41. Hematite sample using 50X zoom microscope.

4.2.2 Hardware/software configuration

The samples described in the previous section have been analysed by means of the RLS ExoMars Simulator in both hardware configurations: with the CompassT and RAD1 spectrometers. Also, data from the RLS FS was used, which had been previously acquired.

Regarding the optical configuration of the simulator, it was necessary to correctly plug the SMA collection optical fiber coming from the Raman probe to the right spectrometer. The CompassT spectrometer can be directly connected to the probe fiber, as it features a female SMA connector. However, an optical

fiber adapter was introduced in the simulator to permit the adaptation of the 200 microns SMA fiber of the ExoMars Simulator probe to the 50 microns FC fiber required as input to the RAD1 spectrometer. It is obvious that the presence of the adapter introduces light losses (if the adapter is ideal the losses suppose $^1/_{16}$ of the incoming light), which results in much darker spectra. For this reason, a second approach was tested, using two collimators with different focal planes. The results did not vary much and the fiber adapter configuration was used.

All the samples were placed for analysis in the refillable container of the simulator as shown in Figure 42 . In order to ensure a perfect correlation between the analysis of the CompassT and RAD1 spectrometers, the samples were sequentially analysed by both spectrometers without actuating the sample positioning mechanism (but plugging the collection optical fiber to the right spectrometer).
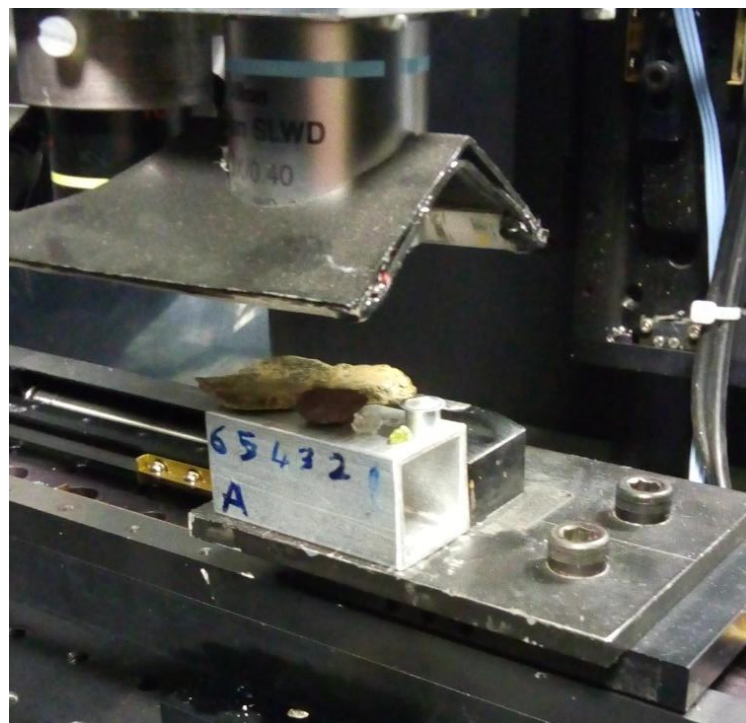
Figure 42. Minerals under analysis behind the optical head.

Universidad de Valladolid

4.2.3 Data acquisition

The analysis philosophy consisted on the acquisition of 200 spectra of 1 accumulation on the one point of each sample with both spectrometers. The integration time for the vast majority of minerals was set to 5 seconds. Nonetheless, for obscure materials such as the Hematite with the RAD1, the integration time was incremented to acquire clear spectra. Laser power has been also modified according to the material under analysis. The majority of samples have utilized a power set to 30%, which provides a similar power on the sample to the one provided by the real RLS instrument. Nevertheless, depending on the samples and detection capabilities of the instruments, the parameters were adjusted by performing a preliminar manual analysis on the sample spot to obtain the best possible results. The full set of parameters detailed by sample and spectrometer are gathered in Table 2.

	CompassT		RAD1	
	Integration time (s)	Laser Power (%)	Integration time (s)	Laser Power (%)
Calcite	5	30	60	90
Diamond	0.12	30	5	30
Hematite	15	40	60	40
Olivine	5	30	5	90
Vermiculite	15	30	60	90

Table 2. Acquisition parameters for each sample and spectrometer.

4.2.4 Data analysis

4.2.4.1 Spectral range and resolution

For the calculation and analysis of the Spectral Resolution, the SpectPro software has been used. This software is being developed by the researchers of the Associated Unit UVa-CSIC-CAB for the exploitation and analysis of spectra acquired by the RLS instrument, including tools such as SNR calculator, Baseline removal, zooming or labelling, spectra normalization and filtering, spectra calculation or tools for peak detection and band adjustment. Figure 43 displays the SpectPRO-IDAT interface with the Calcite sample captured with the CompassT spectrometer as an example of the utilization of the software.
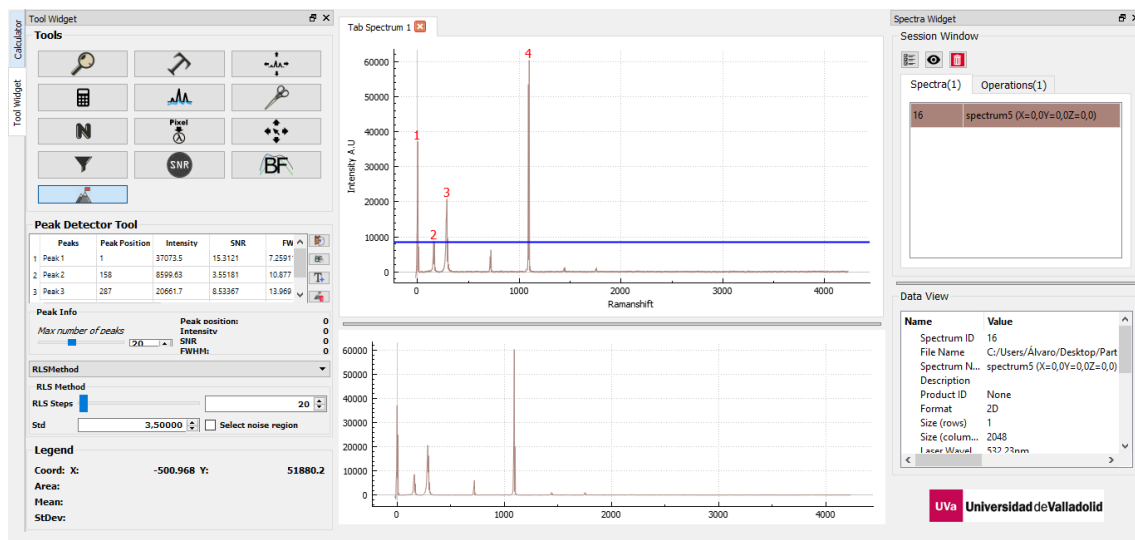
Figure 43. SpectPRO-IDAT interface, displaying the Calcite acquired with the CompassT spectrometer.

In this way, for the particular analysis developed in this project, Baseline elimination and peak detection (provides directly the FWHM) functionalities of the software have been used to study the Spectral resolution obtained with each instrument.

4.2.4.2 SNR evolution with accumulations

The SNR can be defined rigorously as the inverse of the relative standard deviation of the measurement (*Raman Spectroscopy for Chemical Analysis - Richard L. McCreery*, n.d.). Equation 3 shows the way to calculate the SNR, considering $\bar{S}$ as the peak height averaged divided by the standard deviation (σ_y) of the peak height.

$$SNR = \frac{\bar{S}}{\sigma_y}$$

Equation 3. SNR mathematical definition.

However, typically the SNR in the rigorous definition is not as useful to provide an idea of the spectral quality of the spectrum, but of the acquisition device (as it measures the peak intensity variation along several acquisitions). In day-life use of Raman spectra, an alternative SNR definition is used, which compares the main peak intensity with respect to the standard deviation of a region of the spectrum with no peaks. This way it is possible to evaluate the capability to distinguish a peak from the spectral random variations or noise. In our evaluation, the SNR is calculated using the SNR differential method. This particular method uses the difference between two spectra (i.e. it calculates a noise spectrum, and the method is labelled Method 2 because of this) to calculate the standard deviation of the noise in a determined *noise region*, while the intensity is calculated as the maximum value of the peak with respect to the baseline, defined in a determined spectral region, the *peak region*. This SNR calculation has the advantage of not considering the inherent uncertainty introduced by baseline correction methods. On the other hand, the effectivity of the method is compromised due to the need of using two spectra to calculate the noise spectrum, reducing the effective number of available spectra for analysis.

With this calculation method the standard deviation (σ_y) is divided by $\sqrt{2}$ after each accumulation (Raman Spectroscopy for Chemical Analysis - Richard L. McCreery, n.d.), thus reducing the weight of the noise in the SNR calculation.

However, given that the calculations in this work are intended to be compared among the different instruments and samples, this scaling factor does not constitute an issue.

Table 3 provides a summary with the different noise and signal regions used to calculate the SNR of each material. These regions have been selected according to the spectral characteristics of each sample in a preliminary analysis of the spectra (represented in Figure 44 and Figure 45).

	CompassT		RAD1	
	Signal Region (cm⁻¹)	Noise Region (cm-1)	Signal Region (cm-1)	Noise Region (cm-1)
Calcite	1200-1400	1027-1150	450-650	1027-1150
Diamond	1600-1800	1250-1400	1600-1800	1250-1400
Olivine	1040-1240	778-889	1040-1240	778-889
Vermiculite	800-1000	615-713	800-1000	615-713

Table 3. Signal and Noise range used for the SNR analysis, per sample and spectrometer.

To obtain the calculation of the SNR evolution with the number of accumulations, accumulated spectra are computed using the individual spectra acquired with the simulator, and then used to calculate the SNR with the differential method. The representation of the SNR vs the number of accumulations allows the characterization of the instrument performance for different types of samples.

All the calculations of the SNR values and its evolution are performed using MATLAB.

Universidad de Valladolid

4.3 Results & discussion

This section has been divided into three subsections. The first part provides insight into the gathered spectra with the simulator spectrometers, also discussing some effects and issues encountered during the acquisition. Then, the spectral range and resolution issue is addressed, to finally discuss and compare the SNR evolution of the acquired spectra by the accumulation process.

4.3.1 Acquired spectra

As described in section 4.2.3, 200 spectra were acquired in the different samples with both the CompassT and RAD1 spectrometers. These series of spectra are displayed in Figure 44 and Figure 45. Spectra have been represented and studied, firstly, to evaluate if the collected data is solid and to qualitatively assess the spectral quality. At the same time, they have been used to determine the noise and signal regions of each material (see Table 2) used for the SNR calculation by directly inspecting the spectra.
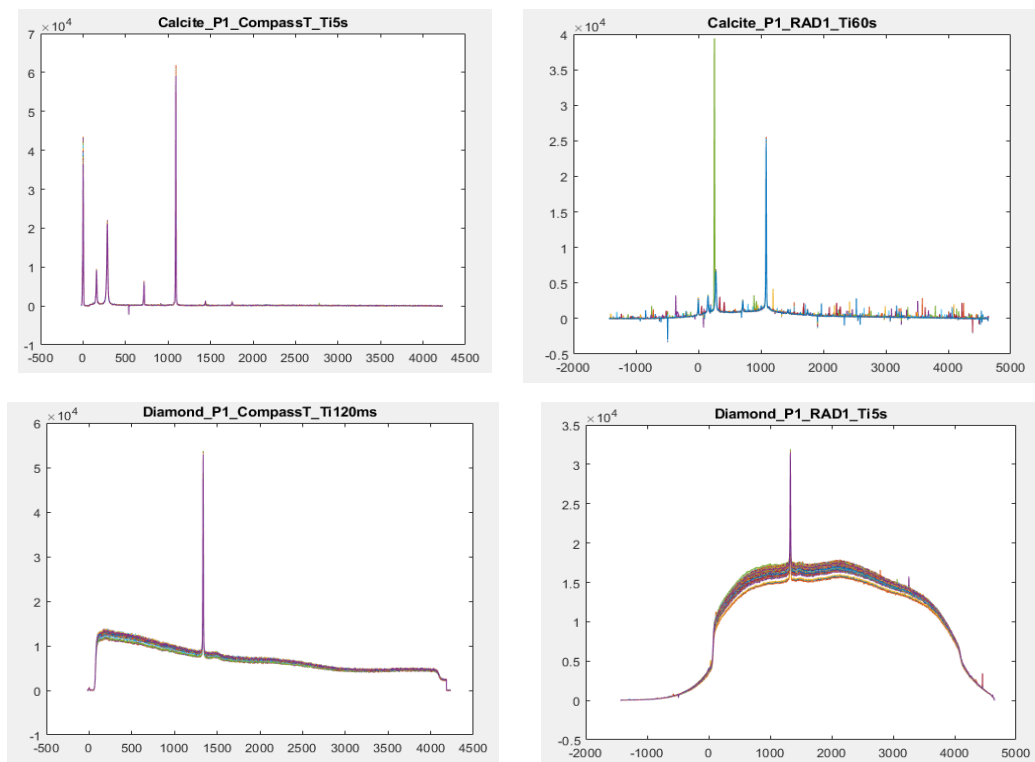
Figure 44. Spectra obtained for each spectrometer (calcite and diamond). Intensity in a.u. (y axis) vs Raman shift in cm^{-1} (x axis).
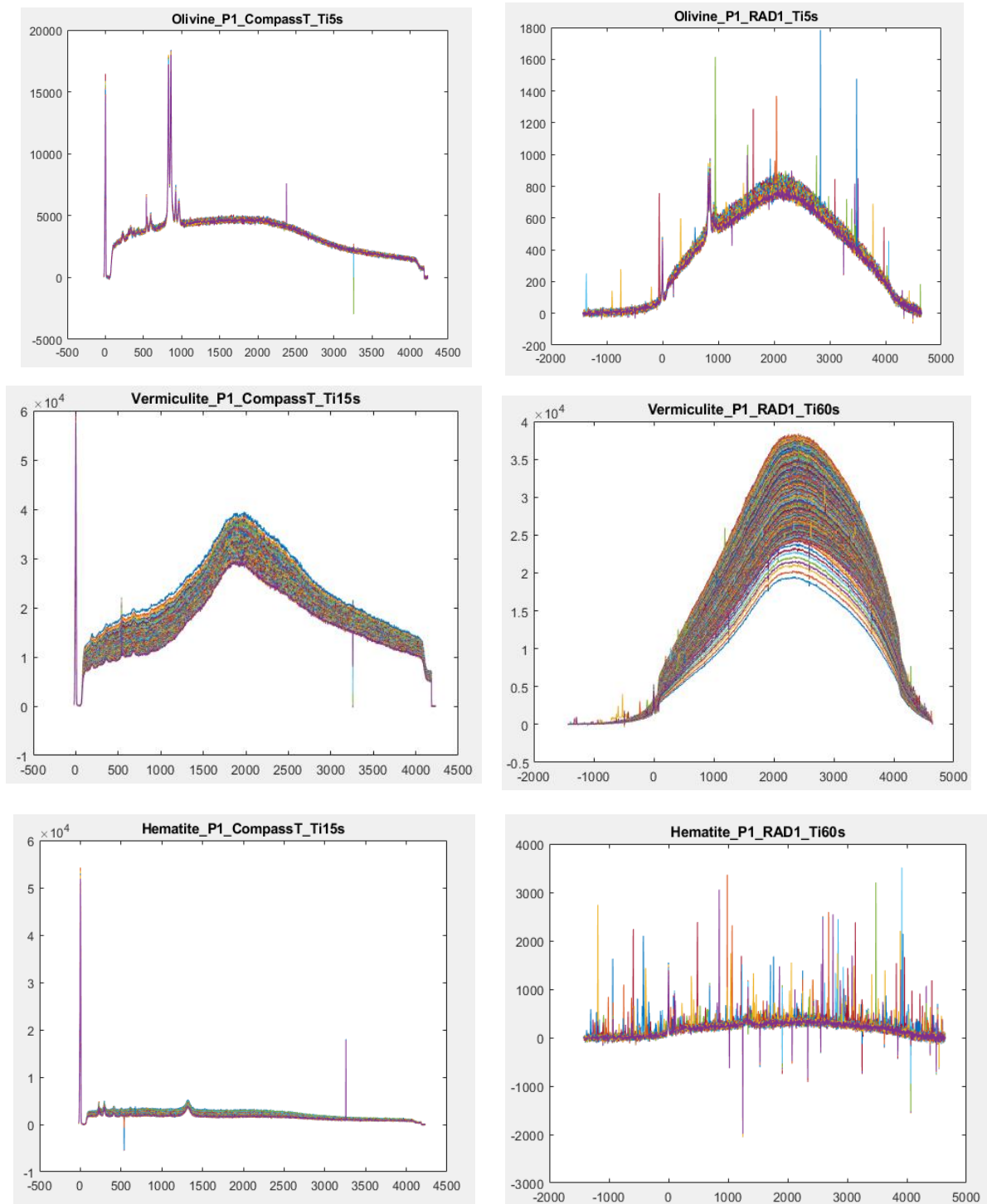
Figure 45. Spectra obtained for each spectrometer (olivine, vermiculite and hematite). Intensity in a.u. (y axis) vs Raman shift in cm^{-1} (x axis).

As can be easily noticed in Figure 44 and Figure 45, the spectra quality is better when utilizing the CompassT spectrometer. This is related to the need to increase the integration time for the RAD1 spectrometer due to the very dark incoming light in the collection path of the RAD1 spectrometer, which has undesired effects on the spectra (see section 4.3.1.2 to 4.3.1.4 for a complete discussion on these issues).

4.3.1.1 Thermolability issues

Thermolability is the sensitiveness to thermal effects that might damage a material. The laser irradiance level on the samples has to be carefully adjusted in terms of power, spot size, atmospheric and temperature conditions, sample status… in order to ensure the safety of the samples. Figure 46 shows the Hematite sample after analysis. Though not obvious, it can be observed in the central part of the image how the sample is not totally focused, which is interpreted as the thermal damage of the laser on the sample (the spot was focused *before* the analysis -though no image is available from before the analysis-).

This thermal damage might be explained by the increase of the laser power to 40%, instead of the typical 30%, together with long analysis times. The idea to increase the laser power is sustained in the need of more laser radiation for this mineral, due to Hematite being a very opaque material and a poor Raman scatterer. Also, during manual preliminary analysis, the sample did not show any significative issue with this laser irradiance level. However, after the automatic acquisition with the Hematite, small signs of burning areas and the obtention of incongruent spectra motivated the decision of not utilizing the Hematite spectra for the SNR evolution analysis.
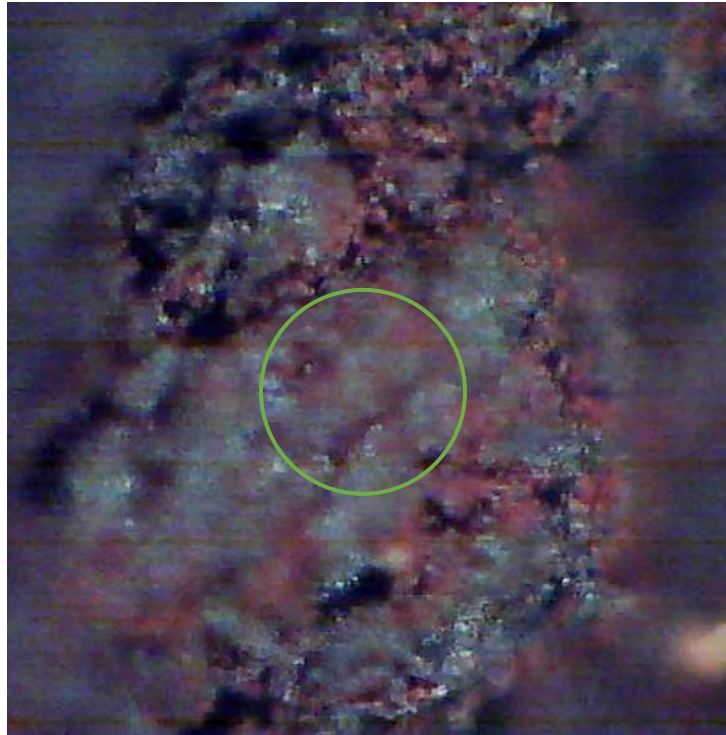
Figure 46. Hematite sample after acquisition, laser area marked in green.

Another example of thermolability can be observed with the vermiculite. Though not especially thermolabile, the before-and-after pictures (Figure 47) of this material showed that the laser had slightly damaged the sample in the central part of the laser spot (where the irradiance level is higher).
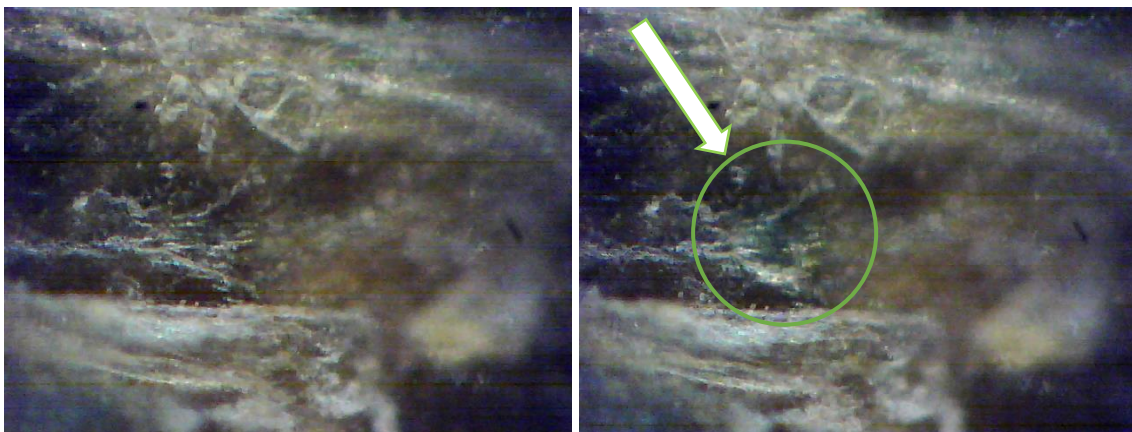
Figure 47. Picture of vermiculite before (left) and after (right) analysis. Green circle shows the approximated spot size of the laser on the sample.

4.3.1.2 Optical configuration issues

Due to the optical fiber adaptation needed to couple the Raman probe collection fiber to the RAD1, as described in the *Materials and Methods* section, the results obtained using the RAD1 spectrometer are much darker than expected with this spectrometer (see Figure 48 as an example with olivine, where same acquisition times with much lower laser power with the CompassT produces a much more intense spectrum than the RAD1 spectrometer, when the RAD1 is more luminous). In order to overcome this issue with the fiber coupling, the integration time and laser power were increased as much as possible with this instrument. These two acquisition parameters are the only possibilities to improve the acquisition without modifying the optical configuration (e.g. using a different Raman probe that can be directly attached to the spectrometer -see Future lines-). On the other hand, this can introduce undesired effects such as damaging the sample or increasing the probabilities of observing cosmic rays or spikes (see next section).
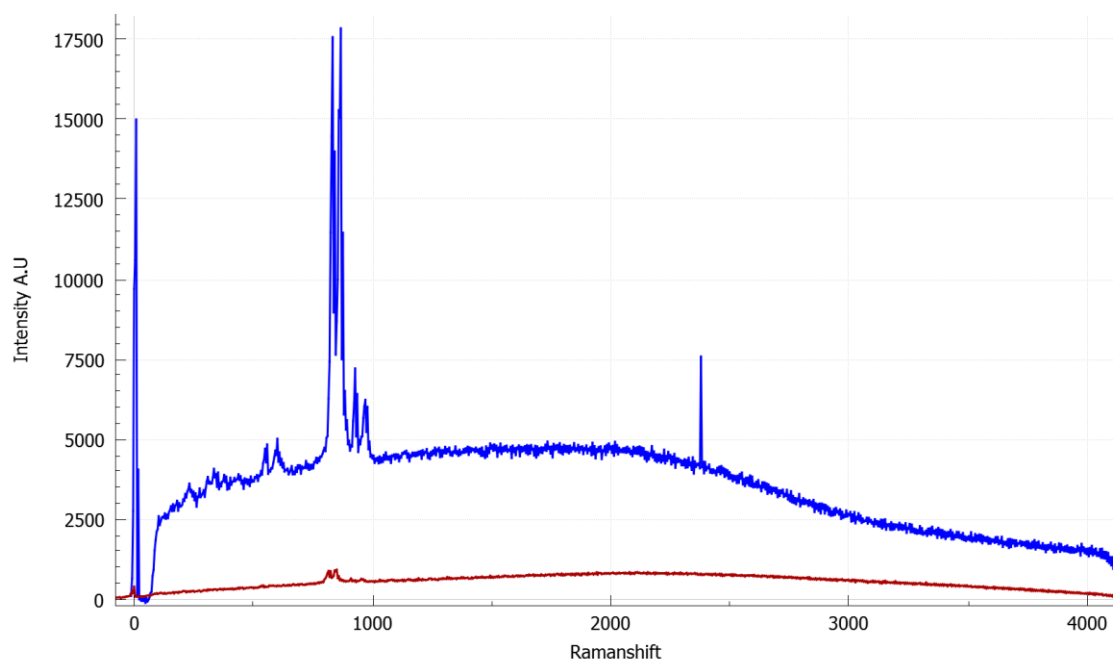
Figure 48. Olivine acquired with the CompassT (blue, Integration time=5s, Laser power=30%) and RAD1 (red, Integration time=5s, Laser power=90%).

4.3.1.3 Cosmic rays and spikes on the RAD1 spectra

Devices based in Silicon, such as CCDs, are affected by high-energy radiation from any kind of source *(Lopez-Reyes & Rull, 2015)*. These events are rare but can affect severely the captured spectrum, because they have enough energy to generate electrons in the surface of the CCD and, thereby, being analysed as photoelectrons from Raman scattering *(Lopez-Reyes & Rull, 2015)*. This effect is expected to be significative in Mars, but on Earth the effect is quite limited.

With respect to this particular study, the presence of undesirable spikes was observed in a few RAD1 spectra. This phenomenon, only appearing in the RAD1 acquisitions, is explained by the necessity to increase the integration time for this spectrometer (derived from the poor optic hitch reached). As a result, the need to use a special MATLAB function (cleanSpuriousFromBatchOfSpectra) to mitigate this effect was implemented. The main differences obtained after using this cleaning function can be seen in Figure 49, where the resulting spectra have successfully been cleaned of many of the spikes.

This function performs a statistical treatment of the data to establish which are the most infrequent peaks at each pixel, assuming that they are spurious to the spectra population. The script calculates the median and standard deviation spectra and considers that all the spectra points found out of the ±3 times the standard deviation (99% of the population) are spurious. For all these points, the spurious value is substituted by the median spectra value is used in the corresponding point.

Universidad de Valladolid
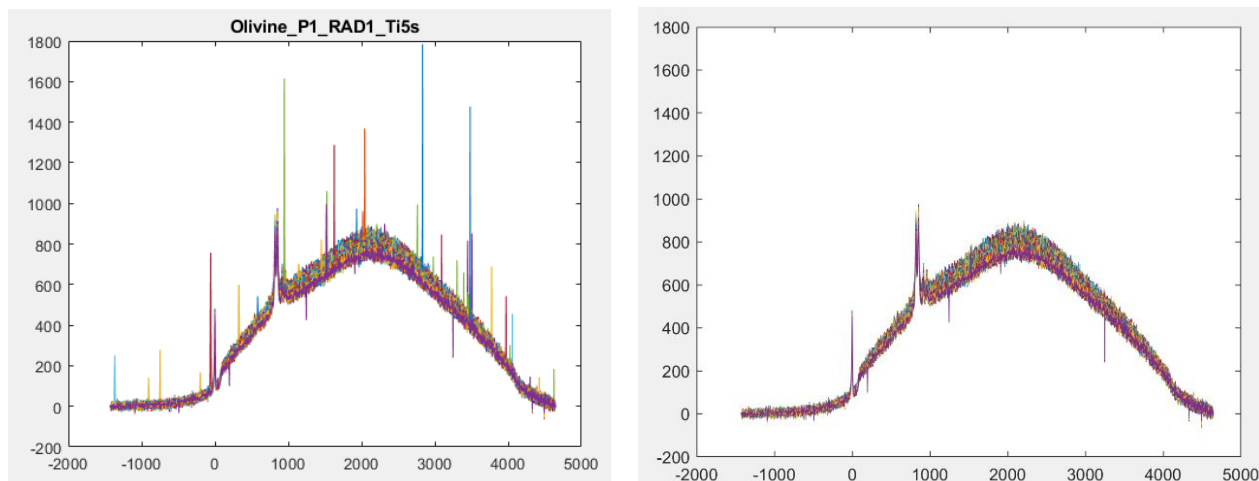
Figure 49. Olivine before (right) and after (left) spectrums utilizing function cleanSpuriousFromBatchOfSpectra.

4.3.1.4 Spectral Calibration

During the study of the acquired spectra, a spectral calibration issue was discovered. The relevance of this problem rests in the necessity of precisely knowing the pixel to Raman shift conversion of the spectral features of the sample under study to assure a subsequent correct interpretation and identification of the detected (but interrelated) concepts: the miscalibration existing between different spectrometer manufacturers and the miscalibration presented with respect to the theoretical wavenumbers. In this case, none of the spectrometers provide a precise Raman shift for the main peaks, which translates into a shift between the spectra (even though the laser emission was properly centered in the 0 position by post-processing. As an example of this calibration issue, the calcite spectra acquired with the CompassT and RAD1 spectrometers. Though this deviation is not critical for the analysis performed in this work, a future line of work was identified to recalibrate the spectrometers.
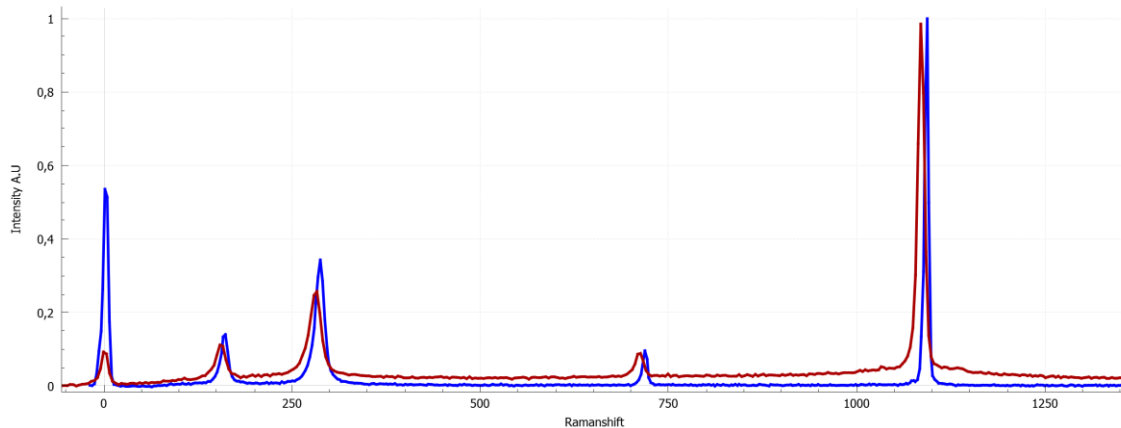
Figure 50. Spectral miscalibration detected in the RAD1 (blue) and CompassT spectrometers (red) on the calcite sample.

4.3.2 Spectral range and resolution

The spectral range and resolution are key parameters to determine the capabilities and quality of the acquired spectra of a spectrometer. The RLS instrument was designed to obtain a theoretical resolution between 6 to 8 cm^{-1} in a spectral range between 0 to 3800 cm^{-1}. This spectral range is amply covered by both the CompassT and RAD1 spectrometer, with spectral ranges expanding further than 0 to 4000 cm^{-1}.

The RLS spectrometer unit complies with the resolution requirement of 6 to 8 cm^{-1}, although experimental results have shown that the resolution might be higher than these values in end-to-end analysis (considering also the laser line emission and the optical head optics).

This resolution, however, enables the procurement of clear spectra, allowing the identification of the principal peak and is also considered enough to resolve partially overlapping peaks. At the same time, this resolution value is wide enough to enable the study of the peak shapes to study other mineral effects (see section *Spectral range and resolution*).

In this context, this section pretends to analyse the results obtained with the two spectrometers of the simulator. For this purpose, the Peak measurement tool of the SpectPro-IDAT programme was used on calcite and diamond spectra

Universidad de Valladolid

(given the intense and narrow emission lines of these materials). The FWHM measurements for Calcite and Diamond are displayed in Table 4.

	CompassT	RAD1
Calcite main peak FWHM (cm⁻¹)	6.05	10.79
Diamond peak FWHM (cm⁻¹)	6.91	12

Table 4. Spectral Resolution in cm^{-1} calculated with SpectPRO.

The CompassT resolution results are clearly better than for the RAD1 and fall into the range proposed for the performance of the RLS instrument. However, as it can be seen, the results of the RAD1 spectrometer fall out of the 6 to 8 cm⁻¹ range, which is anyway in line with the expected results, as the similarity of the optical design of the RAD1 and RLS make the performance of RAD1 spectrometer closer to the RLS one.

The difference in resolution between the RAD1 and CompassT spectrometers can be explained by their different design: the entrance fiber of the RAD1 spectrometer measures 50 microns (representative of RLS), while the CompassT spectrometer uses a 25 microns entrance slit. This allows RAD1 to capture more light while losing some spectral resolution, as the image focusing on the CCD is potentially half for the CompassT compared to the RAD1 spectrometer. Though other factors also influence the final result (optical magnification, CCD pixel size), the entrance slit is the main contributor to this difference.

The other aspect to consider is that the theoretical spectral resolution of 6 to 8 cm⁻¹ established for the RLS instrument is calculated using a lineal emission, considering that the peaks are Dirac delta functions (δ). Taking into account that one of the most narrow Raman emissions is provided by the Island spar (a variety of calcite with a FWHM of the peak around 3-4 cm⁻¹), and that the Raman emission thickness directly adds to the FWHM measurement on a spectrum, it

can be seen how the RAD1 results are not that far from the requirement when subtracting the emission thickness from the measured FWHM values.

4.3.3 SNR evolution as function of accumulations

This section summarizes the different calculations effectuated in order to evaluate the evolution of the spectral quality of the spectra (measured as a function of the SNR) with increasing numbers of accumulations (up to 50). This information is used to compare the performances of the different instruments.

The results are represented in three sets of graphs, with the first set displaying the absolute SNR values (Figure 51, Figure 52 and Figure 53 for the CompassT, RAD1 and RLS FS, respectively); the second providing the relative SNR increase in % with respect to the 1 accumulation spectrum (Figure 54, Figure 55 and Figure 56 for the CompassT, RAD1 and RLS FS, respectively) and the third showing separately the evolution of signal intensity and noise values for detailed analysis and a better understanding of the final SNR evolution (Figure 57, Figure 58 and Figure 59 for the CompassT, RAD1 and RLS FS, respectively). The abscissae axis in all figures displays the number of accumulated spectra.

The SNR data are fitted to an exponential curve. This fit is used as an approximation to the behaviour of the different materials and is used as a tool to reach conclusions and evaluate the general implications of the results.

4.3.3.1 Absolute SNR evolution

The evaluation of the absolute SNR curves (Figure 51, Figure 52 and Figure 53) provides a first clear interpretation: the accumulation process implies a general improvement of the SNR of the acquired spectra. This result is in consonance with the theory, which establishes that accumulating spectra improves the standard deviation of the noise by averaging the random noise components, resulting in better SNR values.

Also, these graphs can be used to compare the absolute SNR values obtained for the different materials and spectrometers. Though the comparison can be biased by the different acquisition configurations (integration time, laser power or even sample position, which is different for the RLS instrument), by comparing the absolute values for one accumulation for the CompassT and RAD1 spectrometers, it is quite clear that the CompassT is performing better (as already discussed in previous sections). In general, the SNR values ratio among the different materials is consistent between both spectrometers, with the exception of diamond on RAD1, which obtains too low SNR values. This is explained by the fact that it was acquired with a relatively low integration time to save operation time (due to restrictions in the access to the laboratory).

The differences that can be observed between the Simulator (CompassT and RAD1) and the RLS FS are mainly related to the calcite SNR values (is much lower in the FS than in the simulator when compared to the diamond). This is explained by the different sample positions analysed. The simulator spectrometers analyse the exact same spot of **bulk** samples, while the RLS instrument analysed the available materials at INTA (powdered calcite). This would explain why the calcite, which provides worse signal when powdered, offers relatively low SNR values with the FS.

4.3.3.2 Relative SNR increment evolution

The examination of the relative SNR increment in % with respect to the one-accumulation spectrum (Figure 54, Figure 55 and Figure 56) offers a better way to compare the SNR evolution for the different samples, as they are represented in the same scale.

The results of are consistent with what it was stated in the previous section. All the configurations offered substantial improvement of the SNR with increasing numbers of accumulations. In these graphs, it draws the attention how the increment percentage of the SNR is much higher in the case of the diamond with the RAD1, while the rest of the minerals maintain similar levels to those shown in the CompassT and RLS FS model configurations. The explanation is again

related to the low integration times used for this acquisition and the access restrictions to the laboratory. Higher integration times increase SNR more than higher numbers of accumulations. However, instead of using a longer integration time to guarantee a good SNR on each spectrum, a relatively short time of 5 seconds (Table 2) was set for the diamond on the RAD1, obtaining poor quality individual spectra for this sample. This implies a low SNR initial value, resulting in a greater quality improvement with the accumulations. Considering this, it can be seen how the RAD1 and RLS FS data behave very similarly for the different materials in terms of SNR increase.

4.3.3.3 Noise and intensity evolution

It is interesting to analyse separately the noise and peak intensity evolutions with respect the number of accumulations (Figure 57, Figure 58 and Figure 59). These figures show how the SNR increase is driven (in general, and as expected) by the noise decreasing when spectra are accumulated: the noise decreases exponentially as shown on the graphs. On the other hand, the peak intensity maintains in general a more or less constant level irrespective of the accumulation number. This is the general behaviour for all the instruments.

One exception that can readily be observed is the vermiculite analysis with the RAD1 which intensity shows a continuous downfall which actually correlates pretty well with the noise decay. This correlation shown between the peak intensity and noise values of the Vermiculite lead to the conclusion that, in reality, Vermiculite graphs were representing the noise, so the peak intensity decreases at the same rate than the noise. A possible explanation of this effect is related to the mineral. Vermiculite is an obscure mineral, a poor Raman scatterer, and slightly thermolabile, making it hard to analyse in general. This, together with the illumination problems of the RAD1 in its current configuration greatly limit the detection capabilities. The future improvements programmed for the RAD1 would hopefully lead to better analysis of obscure minerals such as Vermiculite.
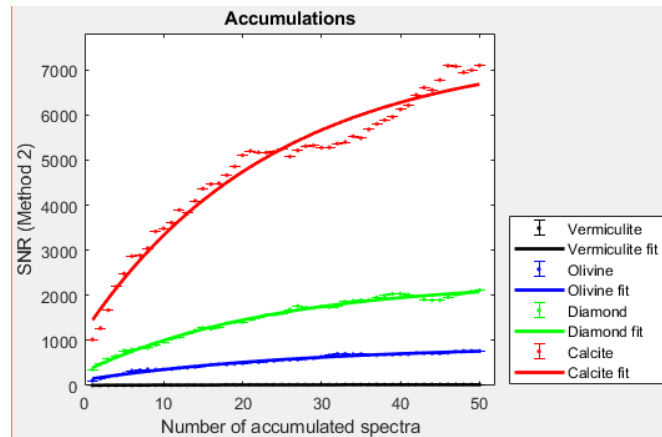
Figure 51. SNR calculation, Simulator (CompassT).
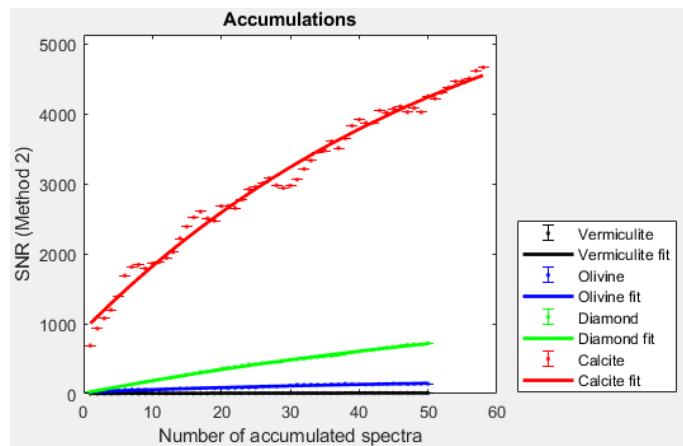
Figure 52. SNR calculation, Simulator (RAD1).
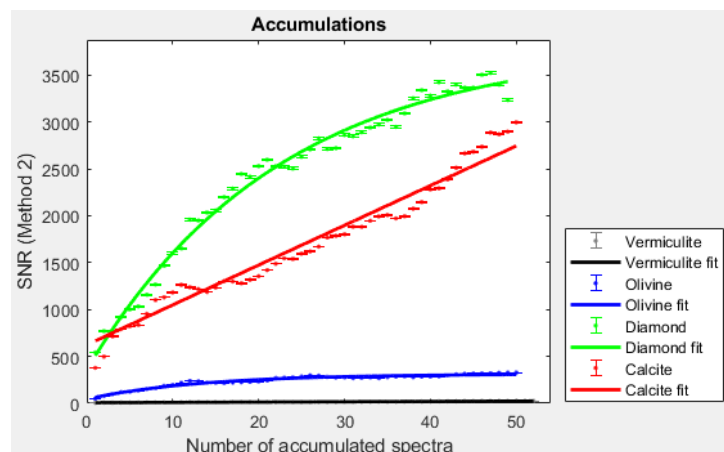
Figure 53. SNR calculation, RLS FS model.
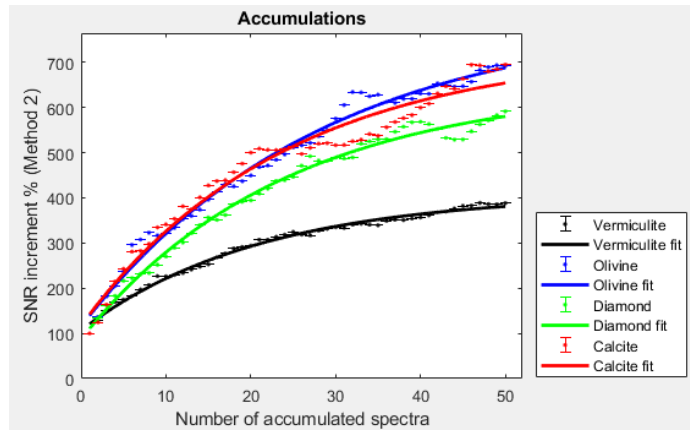
Figure 54. SNR increment % calculation, Simulator (CompassT).
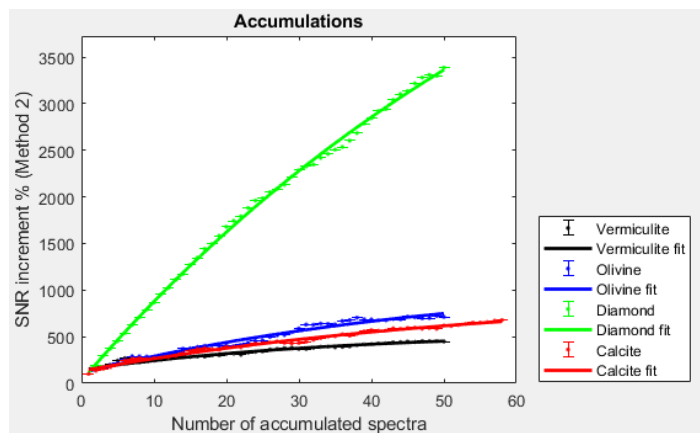
Figure 55. SNR increment % calculation, Simulator (RAD1).
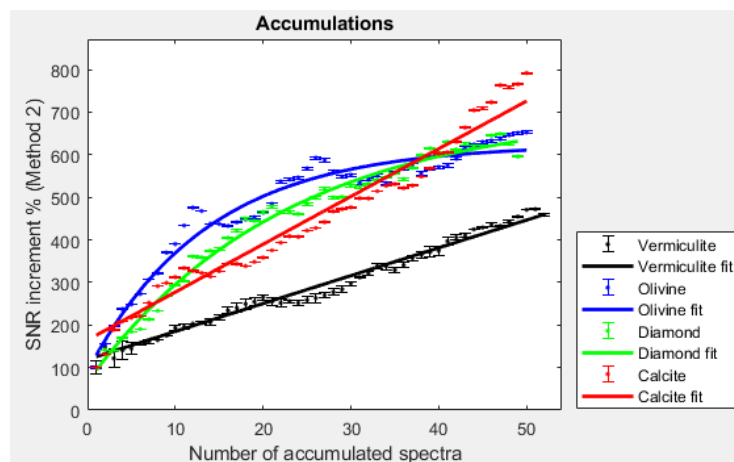
Figure 56. SNR increment % calculation, RLS FS model.
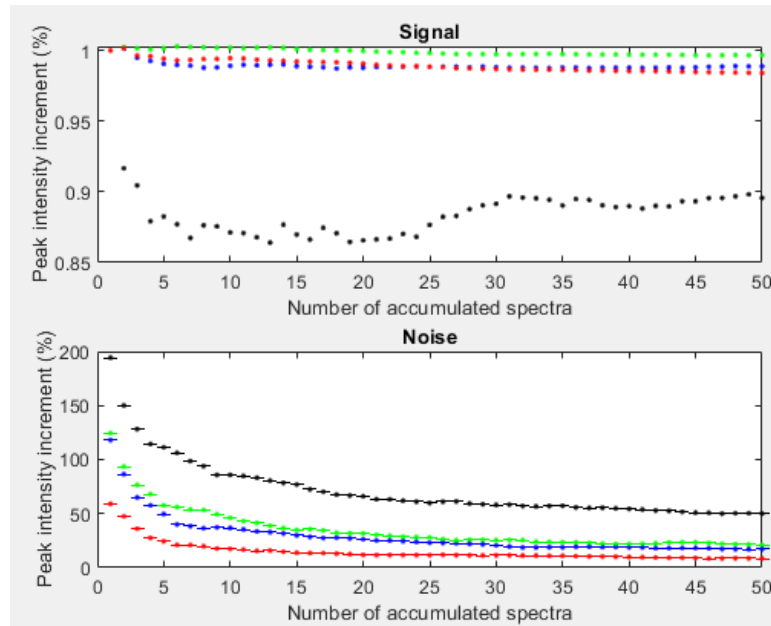
Figure 57. Signal and noise intensity peak increment (%), Simulator (CompassT).
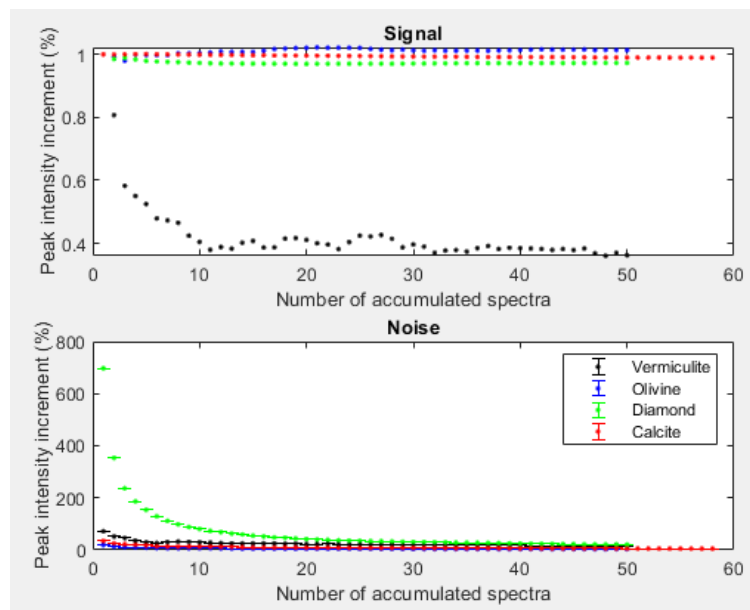
Figure 58. Signal and noise intensity peak increment (%), Simulator (RAD1).
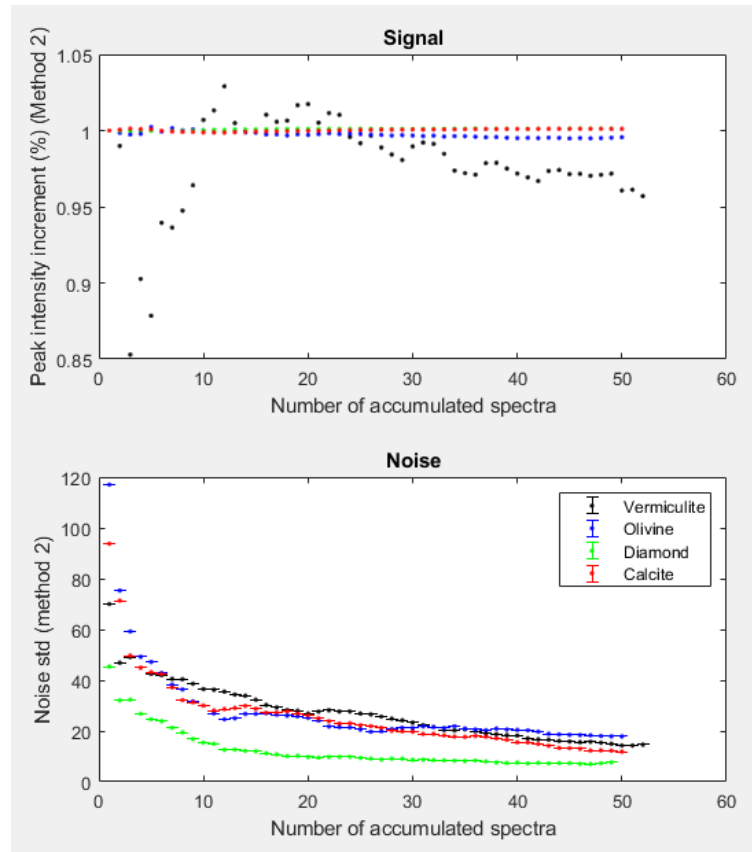
Figure 59. Signal and noise intensity peak increment (%), RLS FS model.

4.4   Conclusions

An analysis performed with both configurations of the RLS ExoMars Simulator has been presented, studying aspects such as the acquisition of spectra on different samples, the evaluation of the spectral resolution or the SNR evolution with the number of accumulations, and their relation to issues such as spectrometer darkness, acquisition parameters, sample thermolability issues or cosmic rays. The objective was to establish a comparison between the behaviour of the RLS instrument and the Simulator in its new configuration with the RAD1 spectrometer.

From this analysis, it can be concluded that the introduction of the RAD1 spectrometer in the ExoMars simulator provides a better approximation to the behaviour of the real instrument, at least comparing with the results obtained with the spare replica (RLS FS model).

Although there are a few differences in results between the RAD1 and the RLS FS model, they are sustained in the different types of samples analysed (bulk vs powder), and also in some undesired issues related to the low light collected by the RAD1 in its current configuration. Indeed, it was observed that the spectra acquired with the RAD1 were much darker than the ones captured with the CompassT. Accordingly, it was necessary to adapt the acquisition parameters (integration time, laser power). This decision enabled the capture of better data from the RAD1, but at the same time, it implied other secondary effect on the CCD such as cosmic rays or thermolability issues.

However, this has also served to identify future lines of work. In a future programmed improvement of the simulator hardware, the introduction of a new optical head will suppose the acquisition of better spectra with the RAD1 spectrometer and resembling even more the real RLS instrument.

5   Conclusions and future work

The "Integration and performance evaluation of the RAD1 spectrometer in the RLS ExoMars simulator" is the work developed for this end-of-studies project. It is developed in the framework of the ExoMars mission of the European Space Agency that will launch a rover on Mars in 2022. In this context, the RLS ExoMars simulator, located in the Associated Unit UVa-CSIC-CAB, is a key device to emulate and simulate the operations of the RLS instrument, a Raman spectrometer part of the payload of the ExoMars 2022 mission.

The work on this project has been divided into three items following the objectives of this work:

- **Learn and understand** the ExoMars project framework, the RLS instrument and Raman spectroscopy, as well as the RLS ExoMars simulator hardware and software. The introduction and state of the art sections have covered a general view of the mission and presenting the contribution of Spain to ExoMars (represented by the UVa-CSIC-CAB and INTA teams), focusing on the RLS instrument and the RLS ExoMars Simulator (hardware and software), while also providing critical insights to Raman spectroscopy, addressing issues such as spectral features or different aspects relevant to the study of Raman spectra.

- **Integration of the RAD1 spectrometer in the RLS ExoMars simulator**: This objective was the main focus of this project. The integration consisted, firstly, in the adaptation of the RAD1 software to make it scalable and compatible with the simulator software. Secondly, the migration and integration process took place, this phase consisting in a general improvement of the software, making it modular, scalable and independent of hardcoded parameters. Then the software critical code involved in the spectra acquisition process was identified, isolated and, finally merged with the corresponding RAD1 code. This process

was done bearing in mind the possibility of future hardware integration activities in the simulator.

This objective of the project is fully covered, as the RAD1 spectrometer is totally integrated into the RLS ExoMars simulator, capturing and analysing data with no important software issues, either in manual or automatic mode. However, a set of improvements were identified that could further improve the overall performance of the RAD1 spectrometer in the simulator.

- **Performance evaluation of the RAD1 spectrometer** in the RLS ExoMars simulator: This last phase of the project, consisted on the study of results obtained with the different configurations of the simulator for validation and test of its performance with the RAD1, comparing it with the RLS instrument, evaluating aspects such as spectral resolution, SNR and SNR evolution with spectra accumulations for different samples with the three spectrometers. The conclusion is that the use of the RAD1 spectrometer with the RLS ExoMars Simulator provides a performance which is more similar to the RLS instrument than its previous configuration with the CompassT spectrometer.

Ultimately, the outcome of the integration and validation of the RAD1 spectrometer into the simulator was satisfactory, reaching the initial objectives regarding the performance improvement of the simulator with the RAD1. Notwithstanding, there is still a few future improvements that have been identified that need to be solved to further approach the performance of the ExoMars simulator to that of RLS, but also to improve the somewhat impaired performance of the RAD1 in the current optical configuration. These future lines of work are listed below:

- CCD temperature check: The monitorization of the CCD temperature during execution would allow the user to check the status of the RAD1 spectrometer at any moment.

- Spectrometer Recalibration: as reported before, it has been noticed that the spectrometers calibrations were slightly deviated between them, but also with respect to the theoretical emissions of the spectra. Thus, a recalibration of both spectrometers is necessary with spectral standards to recalculate the calibration polynomial that converts pixels to Raman Shift, wavenumber and wavelengths.

- Optical configuration related to the Raman probe: A new Raman probe was purchased months ago by the Associate Unit UVA-CSIC-CAB that has not yet been delivered due to the COVID-19 crisis. This probe is designed to allow attaching any optical fiber to it, removing the need for the fiber adaptation from the Raman probe to the RAD1 input fiber. The use of this optical head will mitigate the light losses experienced by the RAD1 spectrometer due to this very inefficient adaptation between the 50 microns FC fiber of the RAD1 and the 200 microns SMA output fiber of the simulator. This change is the most critical, as it will allow the RAD1 to obtain better quality spectrum data.

- Automatic mode algorithms update: The automatic algorithms are the base of the Automatic mode and the activity plan of the simulator and the automated operation of the RLS instrument. Currently, these algorithms are optimized for the CompassT spectrometer, but they need to be optimized for use with the RAD1 spectrometer, also considering other changes in the algorithms operation as implemented on the RLS instrument.

- Integration of a Martian environment chamber: A temperature/pressure chamber will be purchased and integrated into the RLS ExoMars Simulator to allow performing analysis under the conditions of the environment present in the Martian surface. This actualization will further increase the representativity of the RLS ExoMars Simulator.

Universidad de **Valladolid**

(This page intentionally left blank)

(This page intentionally left blank)

REFERENCES

Amer, M. S. (2010). *Raman Spectroscopy, Fullerenes and Nanotechnology*. Royal Society of Chemistry. https://doi.org/10.1039/9781849731133

ESA - Robotic Exploration of Mars - Mars Sample Return. (n.d.). Retrieved July 11, 2020, from https://exploration.esa.int/web/mars/-/44995-mars-sample-return

ESA - Robotic Exploration of Mars - Scientific objectives of the ExoMars Rover. (n.d.). Retrieved July 11, 2020, from https://exploration.esa.int/web/mars/-/45082-rover-scientific-objectives

Ferraro, J. R., Nakamoto, K., & Brown, C. W. (2003). Introductory Raman Spectroscopy: Second Edition. In *Introductory Raman Spectroscopy: Second Edition*. Elsevier Inc.

How do we measure the signal to noise ratio of the Raman spectrometer? (n.d.). Retrieved July 11, 2020, from https://www.researchgate.net/post/How_do_we_measure_the_signal_to_noise_ratio_of_the_Raman_spectrometer

Lopez-Reyes, G., & Rull, F. (2015). Development of algorithms and methodological analyses for the definition of the operation mode of the Raman Laser Spectrometer instrument. *Física de La Materia Condensada, Cristalografía y Mineralogía*.

Ramam Laser Spectrometer (RLS) para Exomars : estado actual Raman en ExoMars y su evolución. (n.d.). 1–30.

Richard L. McCreery, Raman Spectroscopy for Chemical Analysis - (n.d.).

Rull, F., Maurice, S., Hutchinson, I., Moral, A. G., Canora, C. P., Belenguer, T., Ramos, G., Colombo, M., Lopez-Reyes, G., Garcia, V., Forni, O., Popp, J., & Medina, J. (2018). The Raman Laser Spectrometer (RLS) for 2020 Exomars (ESA) Mission: Instrument development and operation on Mars. *EPSC Abstracts*, *12*

Schneider, F. W. (1984). Frank S. Parker: *Applications of Infrared, Raman, and Resonance Raman Spectroscopy in Biochemistry*, Plenum Press, New York and London 1983.

Spectrometer: What is a Spectrometer? | Types of Spectrometers. (n.d.). Retrieved July 11, 2020, from https://www.edinst.com/blog/what-is-a-spectrometer/

Vago, J. L., Westall, F., Pasteur Instrument Teams, Landing S, Coates, A. J., Jaumann, R., Korablev, O., Ciarletti, V., Mitrofanov, I., Josset, J.-L., De Sanctis, M. C., Bibring, J.-P., Rull, F., Goesmann, F., Steininger, H., Goetz, W., Brinckerhoff, W., Szopa, C., Raulin, F., Westall, F., … the ExoMars Project Team. (2017). Habitability on Early Mars and the Search for Biosignatures with the ExoMars Rover. *Astrobiology*, *17*(6–7), 471–510.

W.E.S. (1977). Instrumental methods of analysis. *Journal of Molecular Structure*, *36*(2), 345.

What Is A CCD?- charge coupled device. (n.d.). Retrieved July 11, 2020, from http://www.specinst.com/What_Is_A_CCD.html

What is spectral resolution, and when is it needed? - HORIBA. (n.d.). Retrieved July 11, 2020, from https://www.horiba.com/us/en/scientific/products/raman-spectroscopy/raman-academy/raman-faqs/what-is-spectral-resolution-and-when-is-it-needed/